

ADVANCED STUDY OF VIDEO SIGNAL PROCESSING
IN LOW SIGNAL TO NOISE ENVIRONMENTS

1967 - 1968

BY

Frank Carden
William Osborne
George Davis

A Semi-annual progress report

Submitted to

NATIONAL AERONAUTICAL SPACE ADMINISTRATION
WASHINGTON D. C.

NASA RESEARCH GRANT NGR-32-003-037

Communication Research Group

Engineering Experiment Station
New Mexico State University
Las Cruces, New Mexico

December 1967

ABSTRACT

Part I

A mathematical model for the composite video signal is developed and the results are used to analyze the Apollo TV spectrum. A computer model is developed to generate the spectral components. To use the digital program the brightness function $B(xy)$ must be specified by a 300 by 300 matrix. The computer program converts the spatial brightness function $B(xy)$ into a composite temporal function $V^1(t)$ and gives the spectral components of $V^1(t)$. The spectral analysis showed the computed spectrum in close agreement with the measured spectrum. Further, for the TV pattern investigated the significant spectral components were well below 500 KC; in fact, the components were below the 409 KC sync burst.

Part II

Rice's noise model for Gaussian modulation is modified to represent one mode of operation in the Apollo FM television system and the resulting integrals are solved digitally. A family of threshold curves are plotted with the IF bandwidth the running parameter.

P A R T I

TABLE OF CONTENTS

	Page
LIST OF TABLES	v
LIST OF ILLUSTRATIONS	vi
INTRODUCTION	1
Chapter	
I. TELEVISION SYSTEMS	3
II. STANDARD METHODS FOR ESTIMATING VIDEO BANDWIDTH . .	10
III. THE COMPOSITE VIDEO SPECTRUM	15
IV. GENERAL METHOD FOR OBTAINING THE SPECTRUM OF THE VIDEO SIGNAL	40
V. CONCLUSION	72
APPENDIX	74
REFERENCES	80

LIST OF TABLES

Table	Page
1. Scanning Parameters of the Apollo Television System ..	9
2. Comparison of Calculated Results with Experiment Data for Black and White Pattern	26
3. Comparison of Computer Calculated Results to Mertz and Gray's Analytical Results for a White Circular Test Pattern	57

LIST OF ILLUSTRATIONS

Figure		Page
1.	An Example of Linear Scanning	4
2.	The Apollo Unifier S-Band Television System	8
3.	Construction of a Composite Video Waveform	16
4.	Black and White Test Pattern and Associated Video Waveforms	21
5.	Calculated Amplitude Spectrum for Black and White Test Pattern	22
6.	Detailed Amplitude Spectrum in the Region of the Line Frequency	24
7.	Measured Amplitude Spectrum of the Black and White Test Pattern	25
8.	Envelope of Typical Video Spectrums	29
9.	Diagonal Bar Test Pattern and Corresponding Video Output	33
10.	Envelope of the Amplitude Spectrum for Diagonal Bar Test Pattern	37
11.	Coordinate System Used for the Spacial Fourier Series Expansion	41
12.	Typical Spectrum Showing the Effect of Motion in the Image	46
13.	Computer Calculated Amplitude Spectrum of Video Signal Resulting from a White Circular Image	58
14.	Computer Calculated Amplitude Spectrum for the Diagonal Bar Test Pattern	59
15.	Computer Calculated Amplitude Spectrum Showing Detail About the Line Frequency	60
16.	Computer Calculated Amplitude Spectrum Showing Detail About Fifty Times the Line Frequency	61

Figure	Page
17. Coordinate System Used to Extend Mertz and Gray's Results to Include Composite Video Signals	63
18. The Grate and Gray Scale Test Patterns	65
19. Calculated Composite Video Spectrum Produced by the Grate Pattern	66
20. Measured Composite Video Spectrum Produced by the Grate Pattern	67
21. Calculated Composite Video Spectrum Produced by the Gray Scale	69
22. Measured Composite Video Spectrum Produced by the Gray Scale	70
23. Calculated Composite Video Spectrum Produced by the Logmatic Gray Scale	71

INTRODUCTION

A fundamental problem in the design of any communications system is specifying the bandwidth necessary for transmission of the required information. A television system is no different in this respect than any other communications system. However, estimating the bandwidth of a television system is a more complicated problem than its counterpart in most other communications problems. The basic reason for the added complication is that a television system must transmit a two dimensional picture over a one dimensional channel. The process by which a two dimensional spacial picture is transformed into a one dimensional time series is known as scanning and will be examined in some detail later.

In most communications problems not only is the bandwidth important but the actual spectrum is necessary in order to examine the effect of narrowing this bandwidth. One example of such a problem is transmission of speech over a telephone. The average human has spectrum components in his voice much above 3000 cycles, but by examining these components as compared to those below 3000 cycles, telephone companies have discovered satisfactory reproduction of a normal conversation is possible using a 3000 cycle bandwidth. Thus by examining the actual spectrum of human speech, this industry has conserved valuable bandwidth.

The purpose of this work is to study video spectrums and attempt to answer the question of what is the necessary video bandwidth for satisfactory reproduction and to examine the composite video spectrum. The system of interest throughout this work will be the Apollo downlink television system which will transmit pictures back from the moon during the time that the Apollo astronauts are on the moon. Therefore, all of the numerical results and calculations will be based on this system whereas all mathematical developments will be for a general television system with the only requirements being that it be monochrome and use linear scanning as the method of transformation into the time domain.

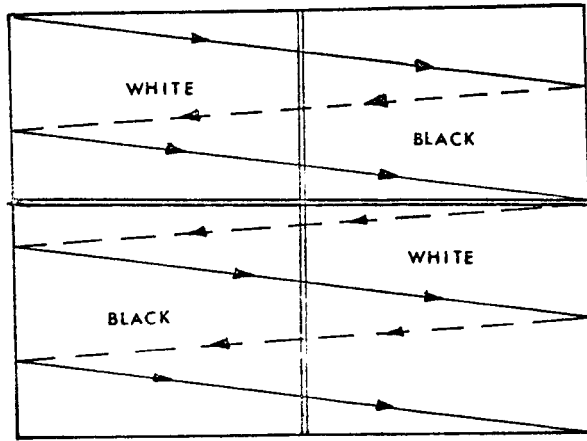
CHAPTER I
TELEVISION SYSTEMS

General Description

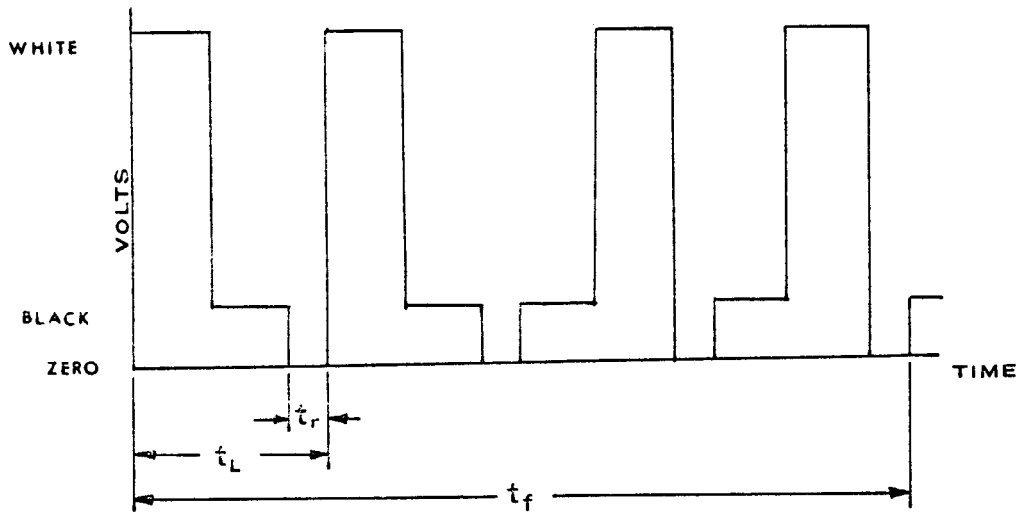
The fundamental purpose of any television system is to transmit an optical image from one place to another by converting it into an electrical signal. The process by which the electrical signal is produced from an optical image is known as scanning. This process forms the basis of modern television systems. There are many methods of scanning an image, but the method most often used is known as straight line or linear scanning. In linear scanning, the optical image is repeatedly swept by an electro-optical transducer whose output as a function of time is proportional to the illumination on the image.

A graphical illustration of this process is shown in Figure 1. The image is a black and white checkerboard pattern and the entire image is scanned with only four lines. Observe that during retrace the output of the transducer, or video, is held at the black level. This is done to prevent the retrace from appearing in the reproduction of the image at the receiver.

Four basic parameters are involved in line scanning--the retrace time, the line scanning time, the frame time, and the number of lines in the scanning pattern. The line scanning time, t_l , is usually not expressed as a time but instead as a



CHECKERBOARD IMAGE SHOWING A SIMPLE 4 LINE SCANNING PATTERN



OUTPUT OF THE SCANNING TRANSDUCER FOR THE IMAGE SHOWN ABOVE

- t_r = RETRACE¹ OR HORIZONTAL BLANKING TIME
- t_L = TIME FOR TRANSDUCER TO SWEEP ONE LINE
- t_f = TIME FOR TRANSDUCER TO SWEEP ONE IMAGE OR FRAME
- $f = 1/t_L$ = THE LINE SCANNING FREQUENCY
- $f_f = 1/t_f$ = THE FRAME FREQUENCY
- N = NUMBER OF LINES IN THE SCANNING PATTERN

ILLUSTRATION OF THE SCANNING PROCESS

Figure 1

frequency, f_{ℓ} , known as the line scanning frequency or simply line frequency. Likewise the frame time, t_f , is usually expressed as f_f , the framing frequency or frame rate. A point of interest is that the line frequency is always a harmonic of the frame frequency. The time to sweep out one frame is the product of the number of lines and the time for one line, or simply $t_f = Nt_{\ell}$. Therefore $f_{\ell} = Nf_f$ where N is always an integer.

At the receiving end of the system, the reverse of this process must be transpiring; i.e., another electro-optical transducer is converting this scanned information into a picture by sweeping across a reproduction device and by varying the intensity or lumination of this device in accordance with the scanned video information being received. However, in order for the picture to appear undistorted, position information must be present in the video signal. This position information is required to lock the scanning spot in the transmitter and the scanning spot in the receiver in perfect synchronization; otherwise, the picture would appear scrambled at the receiver, because the video information would be randomly placed in the reproduced image. This synchronization is accomplished by adding to the video a synchronization signal, which is time multiplexed into the blanking or retrace intervals of the original video signal. This new signal with synchronization added is known as the composite video signal. An example of a composite video signal will be discussed later in conjunction with the Apollo television

system.

The relationship between the scanning parameters mentioned previously and the quality of the received picture is a pertinent problem of television system design. It is also a very difficult relationship to establish, because the quality of a picture is to some extent a subjective term which depends on the human viewer of the picture. However, certain aspects of picture quality may be evaluated quantitatively. One of these is detail in the vertical direction which is directly proportional to the number of lines in the scanning pattern. However, the exact number of lines required for satisfactory reproduction is dependent upon the application. Values from about 200 lines per frame to above 1200 lines per frame have been used.

The frame rate has a dual effect on picture quality. If the frame rate is too low, flicker, the perception of distinct pictures being transmitted, will be apparent to the viewer of the reproduction. A low frame rate will also produce a blurring motion, as will be seen in Chapter IV. However, because the human eye is very perceptive of discontinuities in an image, the frame rate needed to avoid flicker is usually higher than that needed to produce continuous motion.

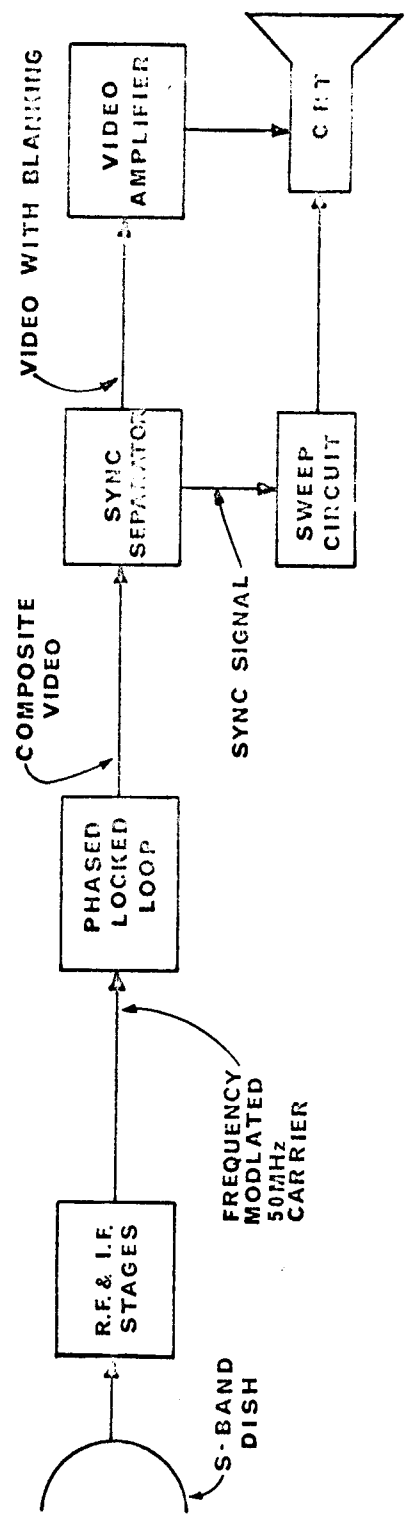
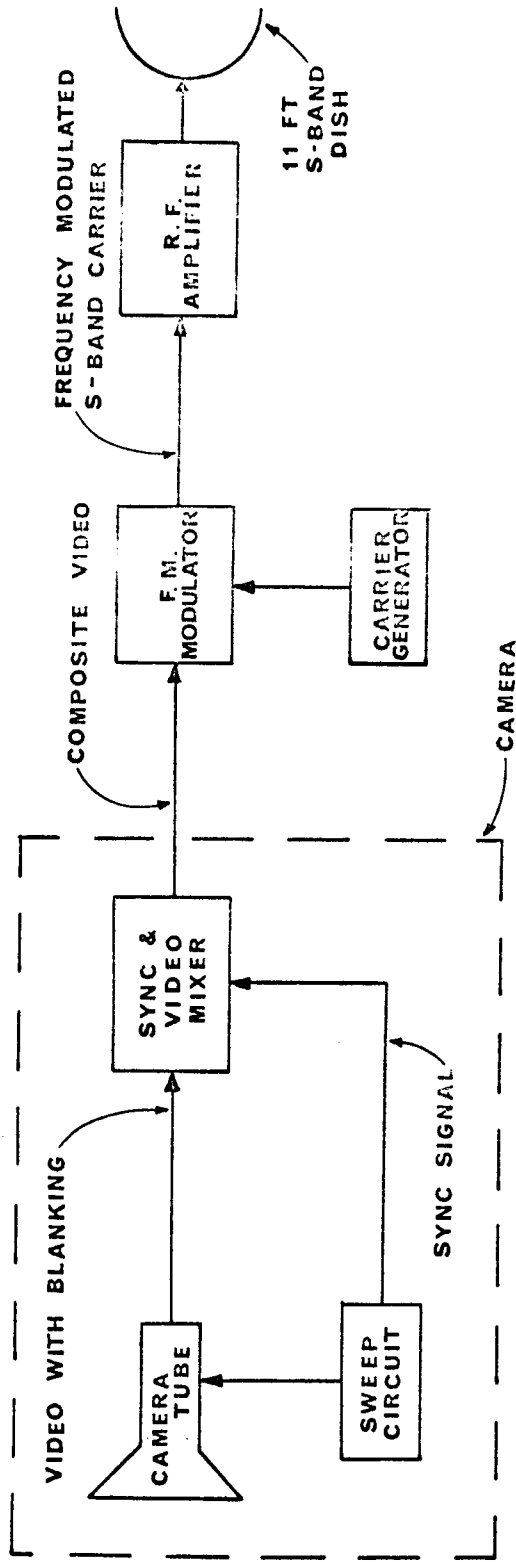
Once a number of lines and the frame rate have been chosen, the line frequency is specified, and the blanking time for retrace, t_r , is then a function of the speed of the pick-up device and the synchronization system used. The relationships between these parameters and bandwidth will be discussed in detail later.

Apollo Unifier S-Band Television System

The television system with which this work is concerned is the Apollo television system for transmitting pictures from the moon. A block diagram of this system is shown in Figure 2. The system consists of a television camera which drives an F.M. modulator to produce a baseband television signal on an S-Band carrier. This F.M. signal is then amplified and transmitted via an eleven foot S-Band dish antenna.

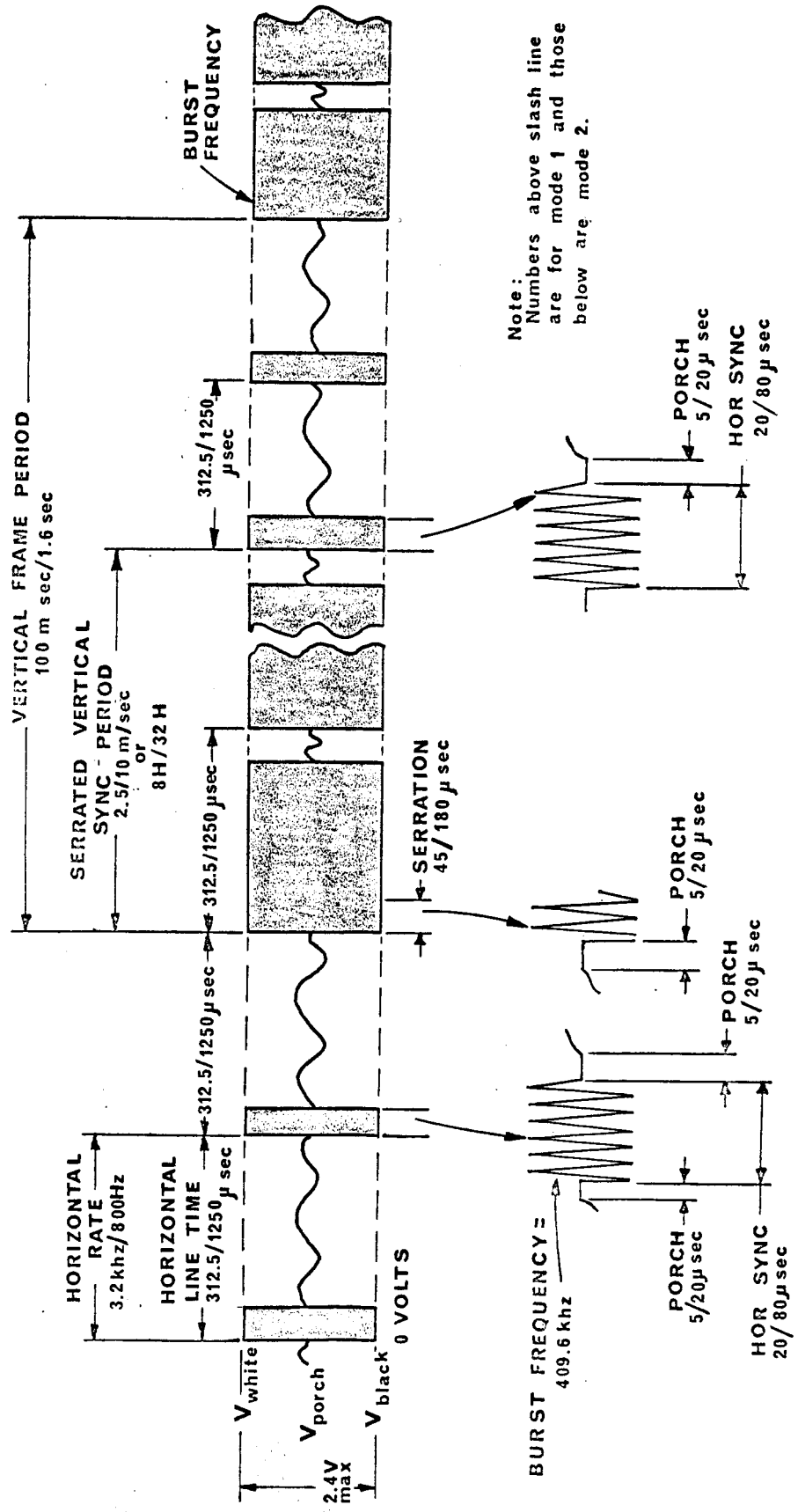
At the receiving station, standard superheterodyne receiving techniques are used to produce a 50MHz frequency modulated intermediate frequency signal. A phased locked loop is then used to detect the signal and feed the detected composite video signal to the synchronization separator circuits. The video and synchronization signals are separated and applied to the picture tube through their respective amplifier and sweeping circuits.

The focal point of this discussion on the Apollo television system is the format of the composite video signal produced by the camera. This format is shown graphically in Figure 2. One of the unique features of this camera is its ability to operate in two modes. Mode one is a fast-scan low resolution mode to be used for transmitting images of objects in motion. Mode two is a slow-scan high resolution mode to be used for transmitting detailed pictures that will comprise a portion of the scientific data to be gathered on the Apollo mission.



**SIMPLIFIED BLOCK DIAGRAM OF THE
APOLLO S-BAND TELEVISION SYSTEM**

Figure 2A



COMPOSITE VIDEO FORMAT FOR APOLLO T.V. SYSTEM

Figure 2B

The synchronization signal consists of horizontal synchronization bursts at a frequency 409.5 KHz and a serrated vertical synchronization burst (See Figure 2) also at 409.5 KHz. The horizontal synchronization occurs during retrace time between lines and the vertical synchronization occurs during vertical retrace between frames. The serrations in the vertical synchronization burst are for the purpose of holding horizontal synchronization during vertical retrace. If these serrations were omitted, the first few lines of each reproduced image would become distorted due to transients in the horizontal sweep circuit of the receiver. The other parameters of the Apollo composite video signal are given in the table below. (1)

TABLE I
Basic Scanning Parameters of Apollo Television System

<u>Parameter</u>	<u>Mode 1</u>	<u>Mode 2</u>
Peak-to-Peak Video Signal	2.4 V	2.4 V
Peak-to-Peak Sync Signal	2.4 V	2.4 V
Horizontal Line Period	312.5 usec	1250 usec
Horizontal Line Frequency	3.2 khz	800 hz
Vertical Framing Period	100 msec	1.6 sec
Vertical Framing Frequency	10 hz	.625 hz
Horizontal Sync Burst Period	30 usec	120 usec
Serrated Vertical Sync Period	2.5 msec	10 msec
Width of Serrations	45 usec	180 usec
Burst Frequency	409.5 khz	409.5 khz
Burst Waveform	Keyed Sinewave	Keyed Sinewave
Number of Lines Per Frame	320	1280
Horizontal Resolution	250 Lines	500 Lines

CHAPTER II

STANDARD METHODS FOR ESTIMATING VIDEO BANDWIDTH

General Discussion

The vertical resolution of a television system is directly proportional to the number of lines in the scanning pattern. The horizontal resolution is a function only of video bandwidth: i.e., the maximum number of vertical lines which may be reproduced is a function of the bandwidth of the system. It should be observed that the bandwidth necessary to achieve maximum horizontal resolution is not necessarily the bandwidth needed to transmit a given image.

There have been numerous methods devised for estimating the required video bandwidth of a television system. However, for the purpose of this work, the author has selected three representative methods which appear most often. All of the methods have two things in common--specifying a worst-case bandwidth which is then used as a design guide-line, and disregarding the actual program material to be transmitted through the system.

Method of Maximum Information

One method of determining the bandwidth of a scanned video signal is to assume that each intersection of a vertical line with a horizontal scan line (using the maximum number of vertical lines) is a sample point. This means that the number of sample points will be the product of the number of horizontal scan lines, N , and the maximum possible number of vertical lines, N_h . Then

each of these sample points may be considered quantized into eight levels. It has been shown that eight quantizing levels will represent an actual analogue television signal with reasonable accuracy. (2)

The channel capacity necessary to transmit any signal is equal to the maximum rate of transmission of information. If n symbols are assumed to occur with equal probability and each takes an identical time, t_t , to transmit, then it has been shown (3) that the necessary channel capacity, C' , is

$$C' = \frac{\log_2 n}{t_t} \quad \text{bits/sec.} \quad (1)$$

For a television system, the n symbols become the eight words necessary to represent the amplitude of a sample, and if the eight words are assumed to occur with equal probability, then Equation 1 is applicable to such a system and the channel capacity of such a television system is given by Equation 2.

$$C' = \frac{3}{t_t} \quad \text{bits/sec.} \quad (2)$$

Now the time required to transmit each sample is the number of samples divided into the vertical framing period of

$$t_t = \frac{1}{f_f N_h} \quad \text{bits/sec.} \quad (3)$$

Thus the channel capacity required to transmit the assumed signal is

$$C' = 3f_f N_h \quad \text{bits/sec.} \quad (4)$$

The appropriate relationship between bandwidth and channel capacity in a noisy channel has been shown to be (4)

$$C' = BW \log_2 \left(1 + \frac{S}{N} \right) \text{ bits/sec.} \quad (5)$$

The signal to noise ratio for high quality image reproduction has been shown to be approximately thirty. (5) Using this value and Equation 4 in Equation 5 and rearranging, the system bandwidth becomes

$$BW = .6 f_f N N_h \text{ hz.} \quad (6)$$

Using the parameters from Table 1 in Equation 6, an approximation to necessary bandwidth for the Apollo system is obtained as

$$BW (\text{mode 1}) = (.6) (10) (312) (250) = 468 \text{ khz.}$$

$$BW (\text{mode 2}) = (.6) (.625) (500) (1248) = 247 \text{ khz.}$$

Method of Vertical Bars

In using this method for determining the required system bandwidth, an image consisting of nothing but vertical bars of alternating black and white illumination is assumed. It is further assumed that these bars are of width h/N_h where h is the horizontal width of the picture. Thus the system is being required to operate at its maximum horizontal resolution.

When this type of image is scanned, the ideal video output

is a square wave with a period of $2t_l/N_h$ and a fifty percent duty cycle. The assumption is then made that for the purposes of reproduction, a sinewave of this period is sufficient. (6)

Thus, the required bandwidth based on this type of analysis is given by

$$BW = \frac{N_h}{2t_l} \quad \text{hz.} \quad (7)$$

The necessary bandwidth for the Apollo television may be calculated using Equation 7 and parameters from Table 1.

$$BW \text{ (Mode 1)} = \frac{210}{2(282.5) \cdot 10^{-6}} = 380 \text{ khz.}$$

$$BW \text{ (Mode 2)} = \frac{500}{2(1220) \cdot 10^{-6}} = 205 \text{ khz.}$$

Method of Maximum Rise Time

The output of the scanning transducer when it crosses a vertical black to white boundary is in the ideal case a step function. However, in a real system with finite bandwidth, this step has a rise time which is a function of system bandwidth.

If we assume such a boundary exists, then it follows that the rise time must be less than half the width of one of the minimum width vertical lines used to specify horizontal resolution. The maximum rise time, t_p , based on the above discussion becomes

$$t_p = \left(\frac{1}{2}\right) \frac{t_l}{N_h} \quad \text{secs.} \quad (8)$$

The upper 3db frequency, f_2 , of a system which will pass a pulse with such a rise time is given by the approximation below which may be found in most texts on video amplifiers. (7)

$$f_2 = \frac{.35}{t_p} \text{ hz.} \quad (9)$$

Since the upper 3db frequency is a close approximation to the required system bandwidth, Equations 8 and 9 may be combined to yeild an expression for the required system bandwidth.

$$BW = \frac{.7N_h}{t_l} \text{ hz.} \quad (10)$$

By making use of Equation 10 and the parameters in Table 1, the bandwidth requirements for the Apollo system may be calculated under these assumptions.

$$BW \text{ (mode 1)} = \frac{(.7) (210)}{282.5 \cdot 10^{-6}} = 521 \text{ khz.}$$

$$BW \text{ (mode 2)} = \frac{(.7) (500)}{1250 \cdot 10^{-6}} = 280 \text{ khz.}$$

Another method often discussed in television engineering books is the "Width of Confusion" method. This method was developed by Wheeler and Loughren (8) and yeilds numerical results very similar to the above three methods. However, it makes the assumption that vertical and horizontal resolutions are equal and this is not in general true and is certainly not the case in the Apollo system. Thus it will not be considered in this work.

CHAPTER III

THE COMPOSITE VIDEO SPECTRUM

General Discussion

The video signal produced at the output of a camera, using linear scanning, may be expressed as the sum of two signals-- the total video signal, $v'(t)$, and the synchronization signal, $s(t)$.

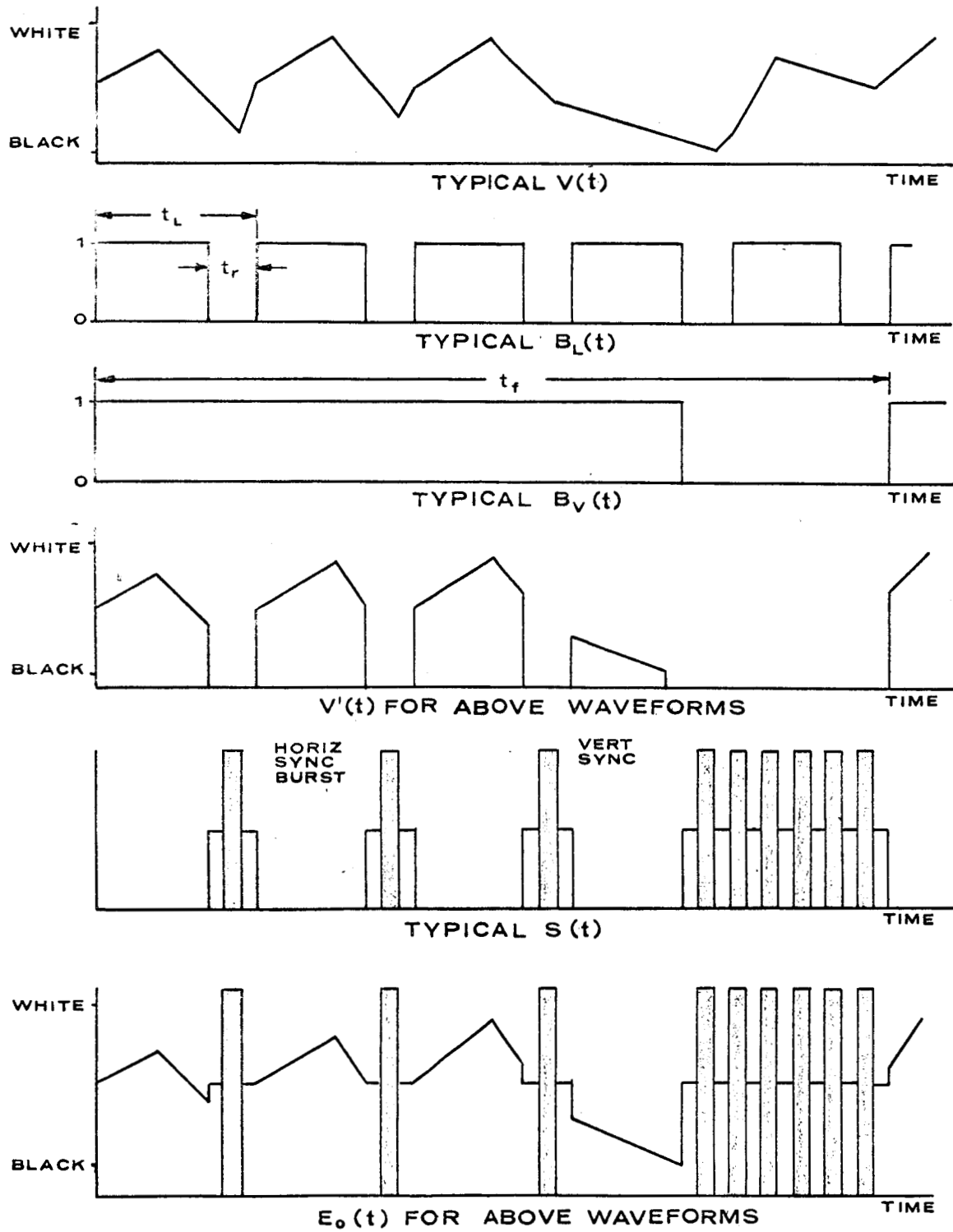
$$E_o(t) = v'(t) + s(t) \quad (11)$$

The total video signal, $v'(t)$, may be expressed as the product of three other functions. One of these is a video signal, $v(t)$, which results from allowing the output of the camera to exist at all times including retrace, or equivalently scanning N pictures placed side by side with no synchronization or retrace interval involved. The second signal is a blanking signal, $B_1(t)$, which is zero during horizontal retrace and one at all other times. The third is another blanking signal, $B_V(t)$, which is zero during vertical retrace and one at all other times. Thus, Equation 11 becomes

$$E_o(t) = v(t) B_1(t) B_V(t) + s(t) \quad (12)$$

This argument is illustrated graphically in Figure 3.

Equation 12 has appeared in an article by L. E. Franks on a random video process, but apparently has not been applied to a deterministic video signal before. (9)



TIME DOMAIN REPRESENTATION
OF A COMPOSITE VIDEO SIGNAL

Figure 3

Development of the Composite Video Spectrum Based on a Time Series

Model

Using Equation 12 as a starting point, the composite video spectrum may now be developed. The blanking function, B_v , represents a square wave with a very high duty cycle and narrow spectrum and, for that reason, neglecting this function has no significant effect on the spectrum of $E_o(t)$. (10) Making use of this approximation, Equation 12 becomes

$$E_o(t) = v(t) B_l(t) + s(t). \quad (13)$$

$E_o(t)$ is the time representation of the composite video signal as it occurs at the output of the camera, and, therefore, its spectrum is the spectrum to which the remainder of the television system must respond. The spectrum of $E_o(t)$ is given by the two-sided Fourier transform of $E_o(t)$.

$$E_o(\omega) = \int_{-\infty}^{\infty} v(t) B_l(t) e^{-j\omega t} dt + \int_{-\infty}^{\infty} s(t) e^{-j\omega t} dt \quad (14)$$

The second integral is the Fourier transform of the synchronization signal or simply $S(\omega)$. Equation 14 then becomes

$$E_o(\omega) = \int_{-\infty}^{\infty} v(t) B_l(t) e^{-j\omega t} dt + S(\omega). \quad (15)$$

Since

$$E_o(t) = V'(t) + S(t) \quad (16)$$

Then $V'(\omega)$ is given by

$$V'(w) = \int_{-\infty}^{\infty} v(t) B_{\ell}(t) e^{-j\omega t} dt. \quad (17)$$

But $B_{\ell}(t)$ is periodic and may therefore be represented by a Fourier series. Making use of this fact reduces Equation 17 to

$$V'(w) = \int_{-\infty}^{\infty} v(t) \sum_{n=-\infty}^{\infty} B_{\ell}(n) e^{jn\omega_{\ell}t} e^{-j\omega t} dt \quad (18)$$

$$\text{Where } B_{\ell}(n) = \frac{1}{T_{\ell}} \int_0^{T_{\ell}} B(t) e^{-jn\omega_{\ell}t} dt$$

$$\text{And } \omega_{\ell} = 2\pi f_{\ell}.$$

Rearranging Equation 18 yields

$$V'(w) = \sum_{n=-\infty}^{\infty} B_{\ell}(n) \int_{-\infty}^{\infty} v(t) e^{-j(w-n\omega_{\ell})t} dt. \quad (19)$$

The integral in Equation 19 represents another Fourier transform. Making use of this fact, Equation 19 reduces to

$$V'(w) = \sum_{n=-\infty}^{\infty} B_{\ell}(n) v(w-n\omega_{\ell}) \quad (20)$$

Where

$$v(w-n\omega_{\ell}) = \int_{-\infty}^{\infty} v(t) e^{j\omega t} dt \Big|_{\omega=w-n\omega_{\ell}}$$

Equation 20 represents the envelope of the spectrum of the composite video signal.

However, in order to get the actual line spectrum generated by scanning process, it is necessary to consider a still picture. In the case of a still picture being scanned, the video signal, $v(t)$, is periodic at the frame frequency. This is due to the fact that for a still picture, the time domain output of the camera will be identical for each frame. Under these conditions, $v(t)$ is represented by its Fourier series or

$$v(t) = \sum_{m=-\infty}^{\infty} v(m) e^{jm\omega_f t} \quad (21)$$

$$\text{Where } v(m) = \frac{1}{t_f} \int_0^{t_f} v(t) e^{-jm\omega_f t} dt$$

$$\text{And } \omega_f = 2\pi f_f$$

Then making use of Equation 21 and the fact that $B_\ell(t)$ is periodic, $V'(t)$ may be expressed as

$$V'(t) = \sum_{n=-\infty}^{\infty} \sum_{m=-\infty}^{\infty} v(m) B(n) e^{jn\omega_\ell t} e^{jm\omega_f t} \quad (22)$$

Recalling from Chapter I that $\omega_\ell = N\omega_f$, Equation 22 can be reduced

to

$$V'(t) = \sum_{n=-\infty}^{\infty} \sum_{m=-\infty}^{\infty} v(m) B(n) e^{j\omega_f(nN+m)t} \quad (23)$$

Equation 23 is the general expression for the spectrum of the composite video signal resulting from scanning a still image, neglecting the additive term resulting from synchronization.

Application of this Model to a Black and White Pattern

In order to apply Equation 23 to a black and white test pattern, the Fourier transform of $v(t)$ and $B_{\ell}(t)$ must be obtained. In Figure 4, the black and white test pattern is shown with the corresponding $v(t)$ which it produces. The $v(t)$ is a square wave of fifty percent duty cycle with its period equal to t_f . The corresponding $v(m)$ is known to be

$$v(m) = \frac{t_f}{m\pi} e^{-jm\pi/2} \sin \frac{m\pi}{2}$$

The absolute value of this function is

$$|v(m)| = \left| \frac{t_f}{2} \frac{\left(\frac{\sin \frac{m\pi}{2}}{m \frac{\pi}{2}} \right)}{m \frac{\pi}{2}} \right| \quad (23)$$

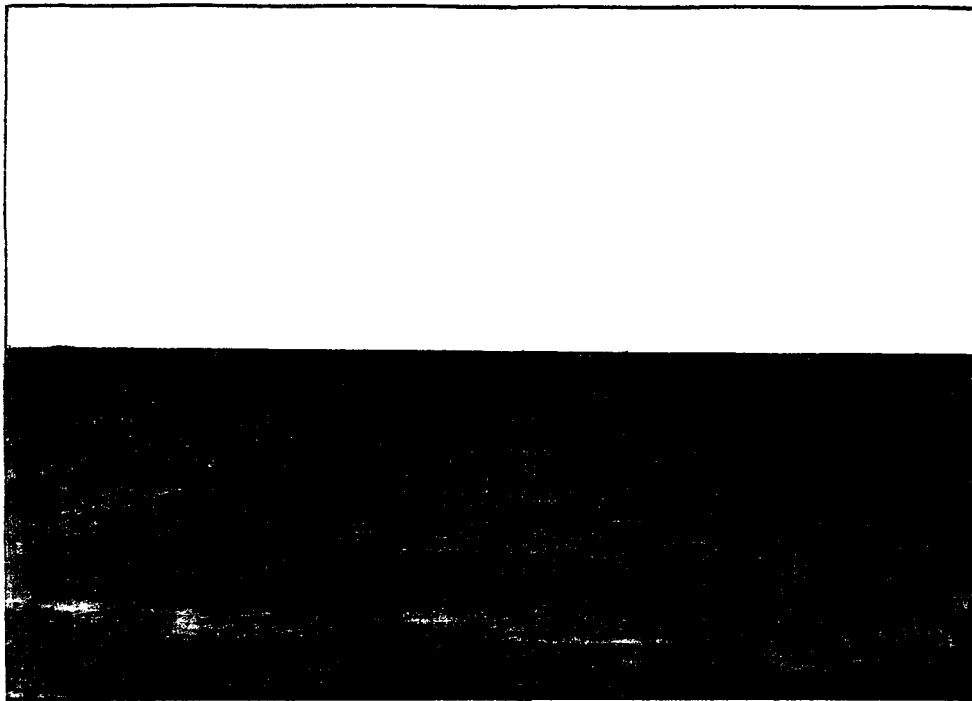
The transform of the blanking signal in Figure 3 is

$$B_{\ell}(n) = \tau e^{-jn\pi\tau/t_{\ell}} \left(\frac{\sin \pi n\tau/t_{\ell}}{\pi n\tau/t_{\ell}} \right)$$

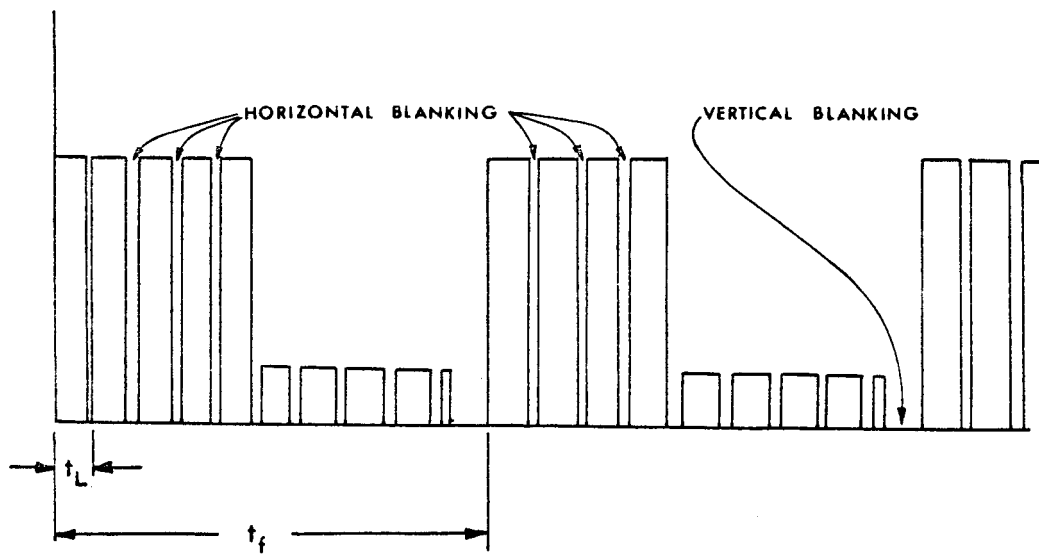
The absolute value of this function is

$$|B_{\ell}(n)| = \left| \frac{\tau \sin n\tau\pi}{t_{\ell}} \frac{1}{\frac{n\tau\pi}{t_{\ell}}} \right| \quad (24)$$

A plot of the product of Equations 23 and 24 versus frequency is the amplitude spectrum of the composite video signal produced by the black and white pattern. This plot is shown in Figure 5 with the amplitude component of the zero frequency term taken as a zero decibel reference. This plot does not show the components about the line frequency harmonics, because such detail is im -



BLACK AND WHITE TEST PATTERN



TIME DOMAIN VIDEO OUTPUT FOR ABOVE IMAGE

BLACK AND WHITE PATTERN

Figure 4

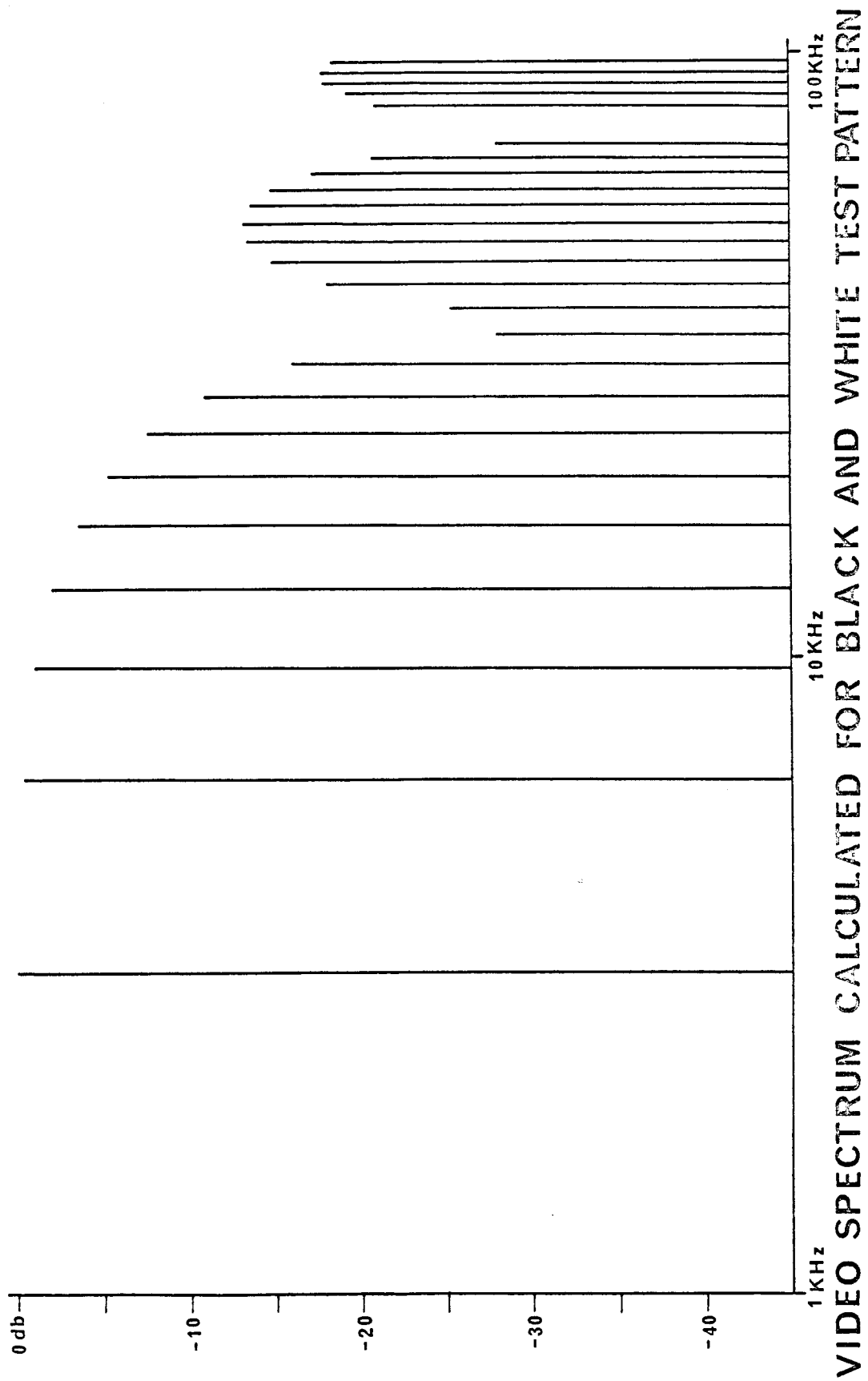


Figure 5

VIDEO SPECTRUM CALCULATED FOR BLACK AND WHITE TEST PATTERN

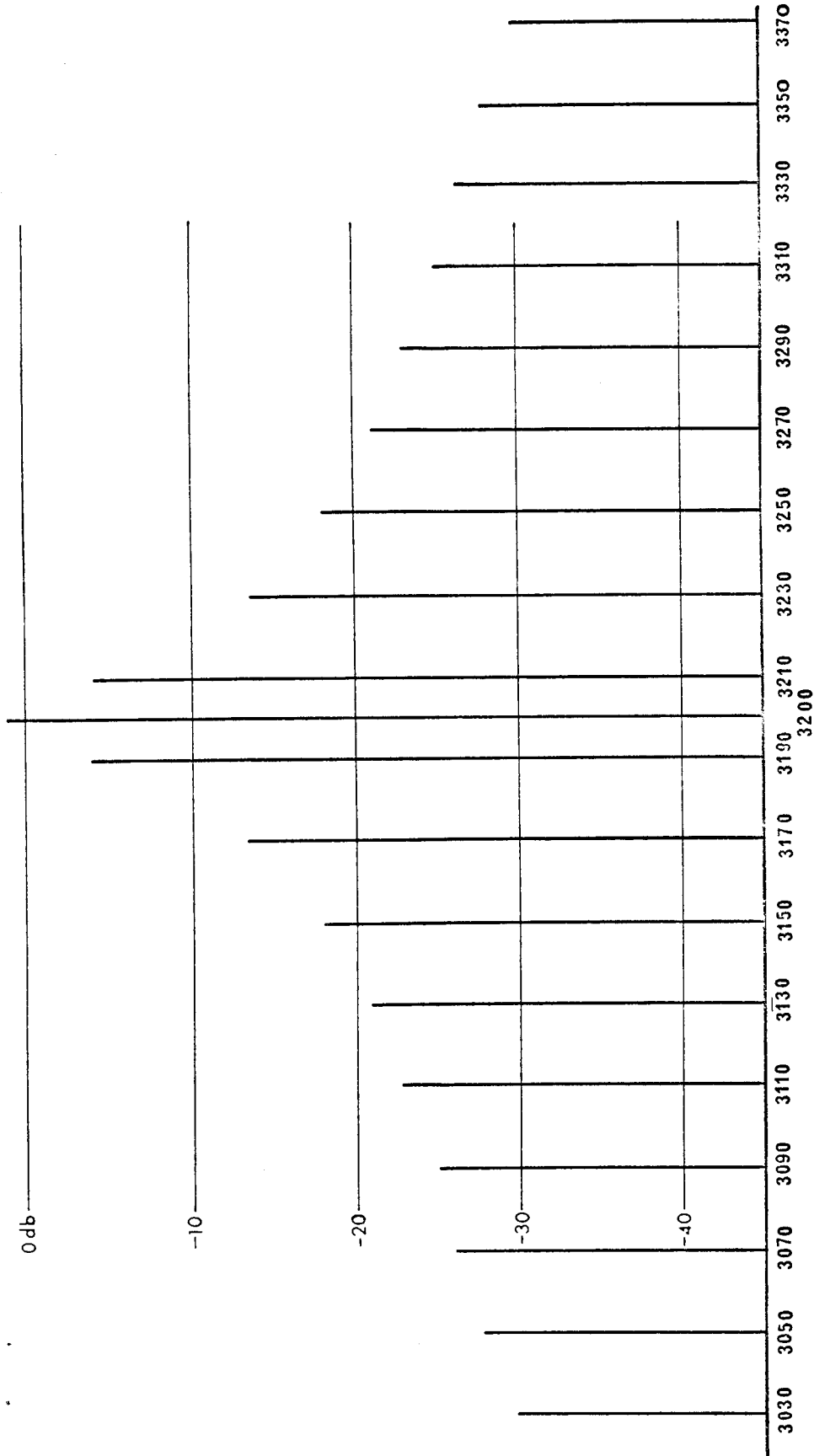
possible to achieve on the frequency scale used. However, this detail has been plotted on a linear scale for the first two harmonics and is shown in Figure 6. In making the plot in Figure 5, the values for τ , t_{ρ} , and t_f were taken from Table 1 and correspond to those to be used in the Apollo television system.

The plot in Figure 5 should be compared with the plot in Figure 7, which is a reproduction of the actual spectrum produced by scanning a black and white test pattern. This spectrum was measured by engineers at the Man Space Flight Center in Houston, Texas. Table II is a comparison of the calculated amplitude spectrum with the measured spectrum for the first twenty-eight harmonics. The agreement between the calculated and measured spectrum is quite good with the average difference being less than 2db, and only four components showing greater than 3db error.

Discussion of the Factors Affecting These Results

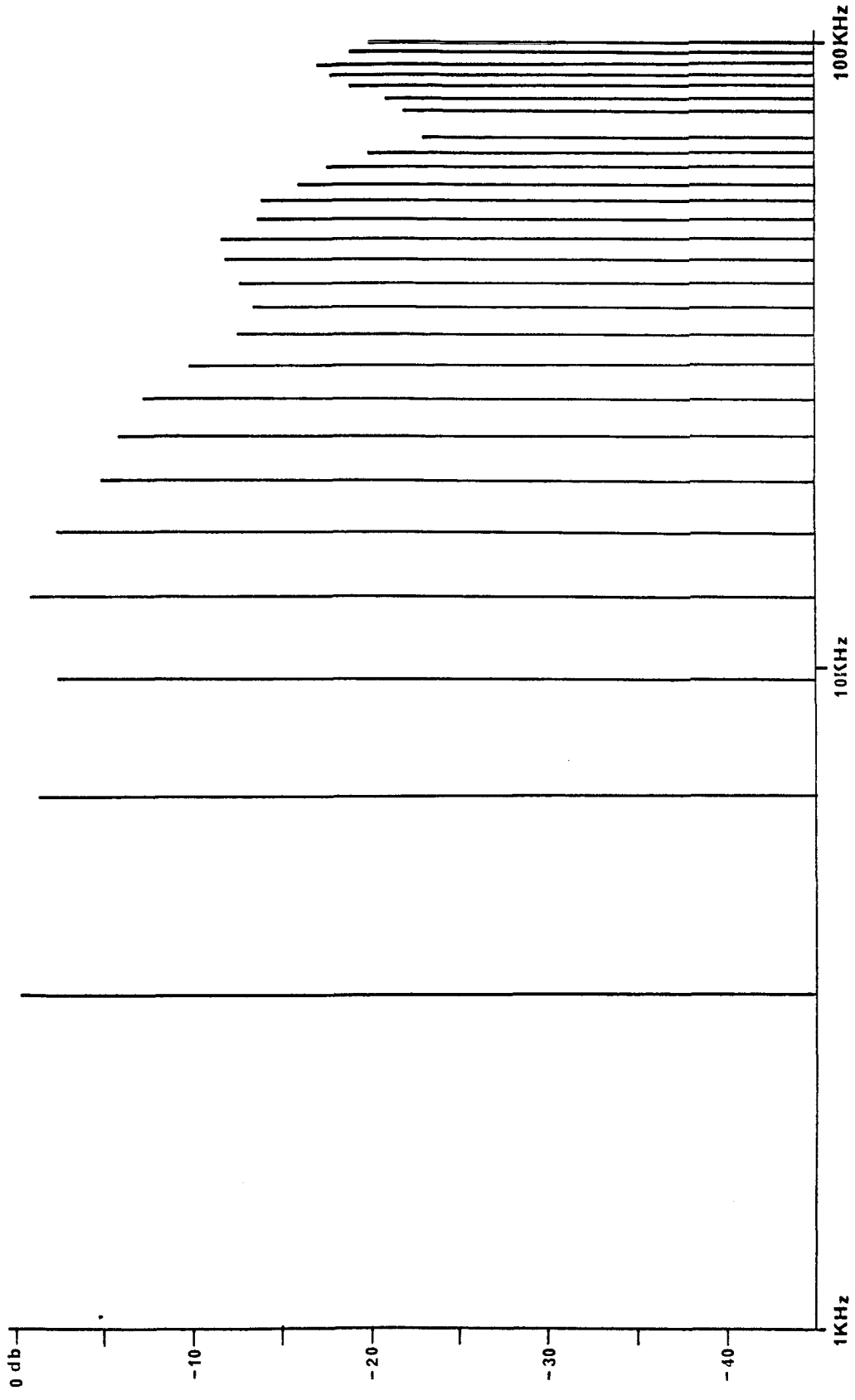
The spectrum resulting from scanning the black and white pattern in the above section is not what is usually expected from an intuitive viewpoint. The basic video signal, $v(t)$, was a ten cycle square wave, yet due to the effect of the blanking signal, this pattern produces components which are only about 40db down from the maximum component at 100KHz. This spectrum is analogous to, but certainly not the same as, the spectrum generated by sampling a bandlimited function. When considered in this light, the result is more intuitively satisfying.

An examination of Equations 23 and 24 reveals some of the parameters which affect this spectrum. From Equation 24, it



**SPECTRUM OF BLACK AND WHITE TEST
PATTERN ABOUT THE LINE SCANNING FREQUENCY**

Figure 6



MEASURED VIDEO SPECTRUM OF BLACK AND WHITE TEST

Figure 7

TABLE II
COMPARISON OF CALCULATED RESULTS WITH
EXPERIMENT DATA FOR BLACK AND WHITE PATTERN

Line frequency Harmonic number, N	Actual Frequency in KHZ	Calculated Amplitude in db	Amplitude Measured by NASA	Difference
1	3.2	-.12	-.4	.8
2	6.4	-.52	-1.5	.98
3	9.6	-1.14	-2.5	1.36
4	12.8	-2.2	-1.0	1.2
5	16.0	-3.6	-2.5	1.1
6	19.2	-5.36	-4.9	.46
7	22.4	-7.72	-6	1.12
8	25.6	-11.04	-7.5	3.5
9	28.8	-16.08	-10	6.08
10	32.0	-28	-12.5	15.5
11	35.2	-25.56	-13.5	13
12	38.6	-18.08	-12.5	6
13	41.8	-14.88	-12	2.88
14	45.0	-13.56	-11.7	1.8
15	48.2	-13.24	-13.8	.6
16	51.4	-13.68	-14	.32
17	54.6	-14.88	-16	1.22
18	57.8	-17.2	-17.7	.5
19	60.0	-20.92	-20	.98
20	63.2	-28.	-23	5.
21	66.4	-48.	not present	--
22	69.6	-26.	-22	4.
23	72.8	-20.92	-21	.08
24	75.0	-19.2	-19	.2
25	78.2	-18	-17.6	.4
26	81.4	-17.8	-17	.8
27	84.6	-18.56	-19	.44
28	87.8	-20.06	-20	.06

can be seen that $B_1(n)$ has an overall distribution of the familiar $\sin x/x$ form and that the parameter which controls the width of the spectrum of $B_\ell(n)$ is τ/t_ℓ , the fraction of time spent for retrace. As this fraction becomes smaller, the first zero of the $\sin x/x$ function becomes greater and the spectral width of $B_\ell(n)$ increases.

From Equation 23, the parameters effecting $v(m)$ may be examined. $V(m)$ also has a $\sin x/x$ distribution and its first zero is given by the reciprocal of the pulse width or the reciprocal of the time interval during which the image is white. For this very special case, this time is $t_f/2$, thus yielding a spectrum of $v(t)$ which is approximately 140 cycles wide. If the transition from black to white had been more gradual going through several shades of gray in between, then $v(t)$ would have had an even narrower spectrum and the frequency components of the composite video would have been much more tightly bound to the harmonics of the line frequency. In the limiting case of a single sine variation from black to white, there would have been only one sideband component for each line frequency harmonic; and it would have been at the framing frequency, 10 Hz.

Changing the test pattern will have no effect on $B_\ell(n)$, since it is a function of the scanning parameters. The effect on $v(m)$, however, may be quite drastic, since $v(t)$ is a function of the picture and of the scanning rates.

In considering the effect of other images on the spectrum of $v(t)$ and thus on the composite video spectrum, it is most

helpful to divide the possible $v(t)$'s into two classes. The first class will be defined as a set of possible images which will generate a corresponding set of $v(t)$'s bandlimited to the bandwidth of $B_\ell(n)$. The other class will be defined as a set of possible images which will generate corresponding $v(t)$'s which have bandwidths in excess of the bandwidth of $B_\ell(n)$. In the case of the Apollo system operating in mode one, this dividing bandwidth for the $v(t)$'s can be taken as approximately 32 KHz. (The first zero of the $\sin x/x$ distribution describing the spectrum of $B_\ell(t)$).

For the class of video functions with their bandwidths limited to the bandwidth of $B_\ell(t)$, the general shape of the spectrum is defined by $B_\ell(n)$. The justification for this statement can best be shown graphically, but before proceeding to such an argument, consider a restricted case of this class of $v(t)$'s. The case is one where $v(t)$ is bandlimited to less than one-half of the line frequency. For such a situation, the composite video spectrum is given by Equation 20. An example of such a case is plotted in Figure 8a. An inspection of this figure reveals that the bandwidth of the composite video spectrum is given by the bandwidth of the blanking signal.

As the bandwidth of $v(t)$ is allowed to increase, the situation becomes more complicated, due to the overlapping of the spectrum of $v(t)$ about each of the line frequency harmonics. An example of this case is shown graphically in Figure 8b. This figure is drawn by considering only five of thirty or forty

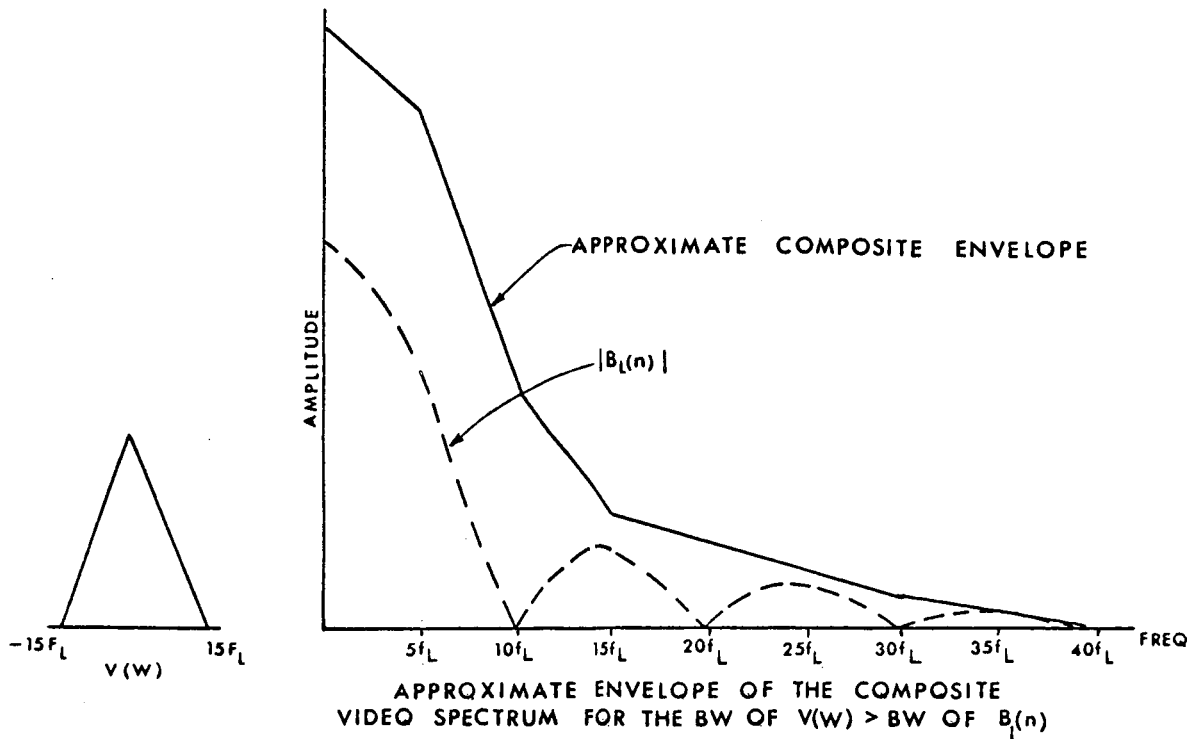
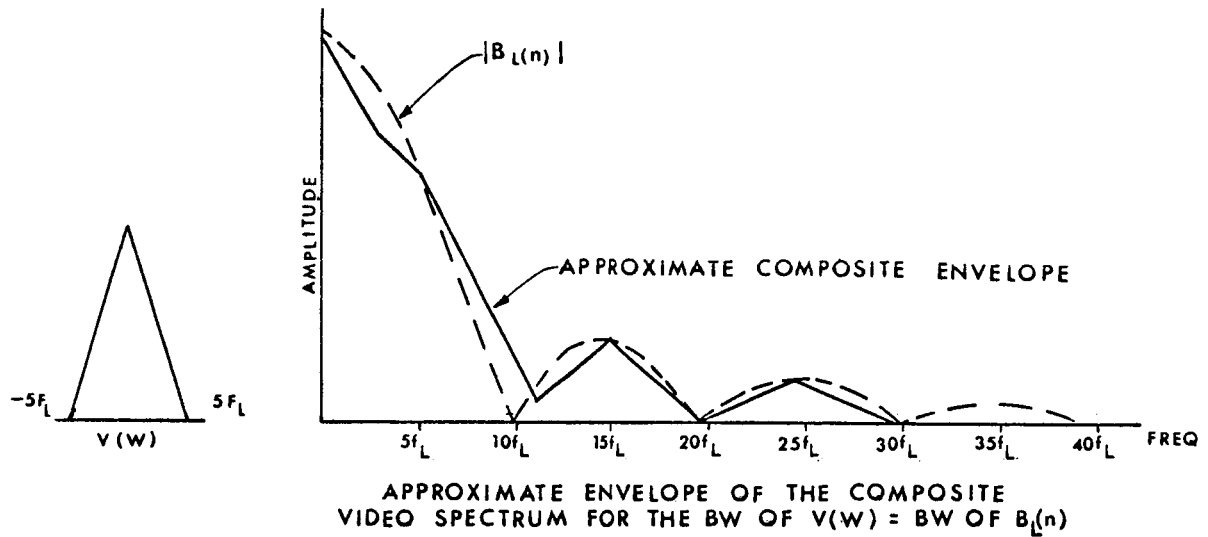
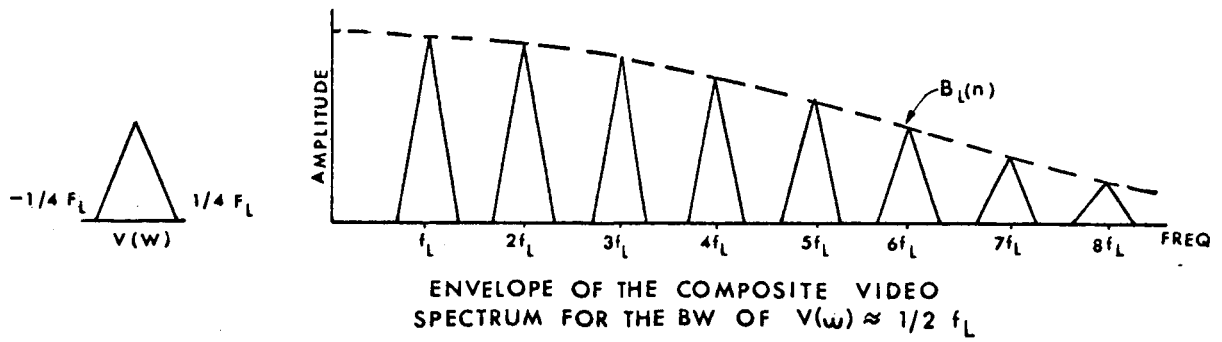


Figure 8

$v(w)$'s displaced about each of the thirty or forty line harmonics given by $B_{\ell}(n)$. $V(w)$ is placed about each line harmonic with the amplitude of $v(w)$ multiplied by the value of $B_{\ell}(n)$ at that harmonic then the envelope of the composite video spectrum was approximated by adding on a point to point basis the envelope of all the $v(w)$'s. Since only five of the $v(w)$'s were considered, this is a fairly crude approximation, but it serves to illustrate the point. A close inspection of Figure 8 will reveal that the harmonics in the upper frequency regions are still very small and that the bandwidth of the composite video signal is still quite close to that of $B_{\ell}(t)$ taken alone. However, the actual fine structure of the composite video signal is no longer easily obtained by this method, since it requires adding all of the components of the various overlapping $v(w)$'s at a frequency to obtain the amplitude of that frequency component.

One point that should not be missed is the fine detail in the region of overlapping. In this region of overlapping, there are no new frequency components generated. This is caused by the unique relationship between the line and frame frequencies. Since the line frequency is a harmonic of the frame frequency and each of the sideband components is separated from the line frequency by multiples of the frame frequency, the overlapping about the line frequency harmonics places sideband components of one line frequency harmonic on top of the sideband components of the next line frequency harmonic. For example, if $v(m)$ has 200 significant components, then the highest frequency term generated

by placing $v(m)$ about f_l is $f_l + 200f_f$, or since f_l is Nf_f , it is $f_f (N + 200)$... However, if N is 250, then this is the same frequency as $2Nf_f - 50$ or the 200th upper sideband component of the first line frequency would fall exactly on the 50th component of the lower sideband of the second harmonic of the line frequency.

The second class of $v(t)$'s presents several new insights; and, in general, when this class of $v(t)$'s is present, then $v(t)$ will be the function which determines the bandwidth and not $B_l(t)$. To begin with, consider the trivial case of $v(t)$ being a unit impulse. Then $v(w)$ is a unity constant over the entire frequency spectrum. Therefore, when such a spectrum is placed in Equation 20 for $v(w)$ and then displaced about each of the line frequencies, it is obvious that the bandwidth of such a spectrum is infinite, because the $v(w)$ placed about the origin extends to infinity with unity amplitude and the other spectrums are only added to this one so that there is no way the blanking signal can limit the bandwidth. The blanking signal will, however, change the constant amplitude, but its effect on this constant amplitude spectrum is a second order one.

As a second example, consider a $v(w)$ bandlimited to about four times the bandwidth of $B_l(t)$, and assume $v(w)$ is a unity constant out to the limiting frequency. A plot of this situation is shown in Figure 8c, once again using only five of the components to obtain the envelope of the spectrum of the composite video. Inspection of this plot reveals that the 3db bandwidth of the

composite video for this case is given exactly by the bandwidth of $v(w)$, and the only effect which blanking has on the composite video spectrum is to raise the level of the very high frequency terms, but they still do not become of the appreciable size.

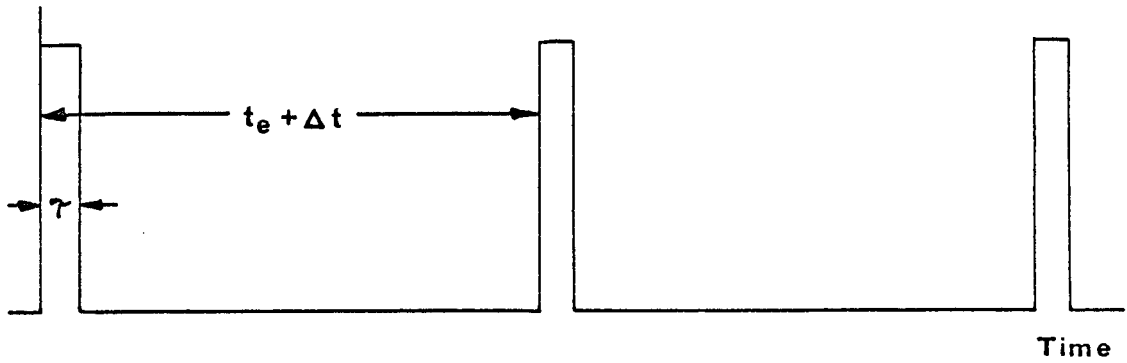
It should be pointed out that the division between the two classes of $v(t)$'s is somewhat arbitrary; i.e., the bandwidth of $B_\ell(t)$ as a division point is not well defined. Rather the situation is that for $v(t)$'s with only low frequency components as compared with $B_\ell(t)$ -- then $B_\ell(t)$ defines the bandwidth of the composite video signal; but for $v(t)$'s with strong high frequency components, then $v(t)$ defines the bandwidth of the system. For the intermediate cases, the bandwidth is greater than either $v(t)$ or $B_\ell(t)$ would indicate, but no simple approximation can be used to find the bandwidth in this case--rather, a plot similar to the ones in Figure 8 seems to be the most straight forward approach.

Determination of a More Complicated $v(t)$

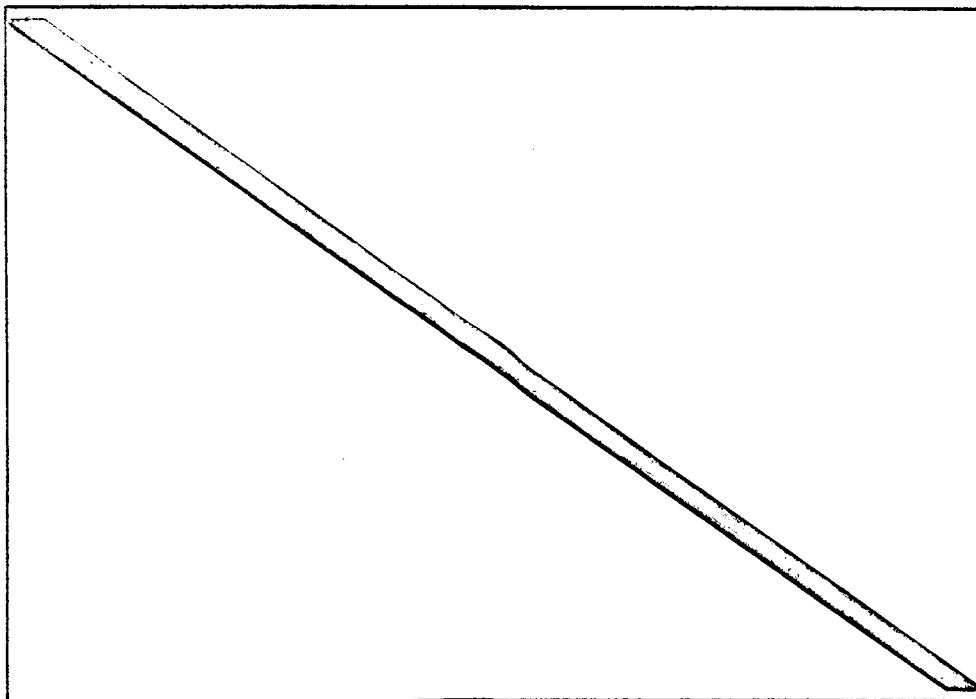
As a final example, consider the video function, $v(t)$ generated by scanning a white diagonal bar on a black background.

The optical image and the corresponding time domain output of the scanning device are shown in Figure 9.

$V(t)$ consists of a series of pulses each of width τ and each periodic at the framing frequency. The spectrum of any one of the periodic pulse trains is given by the Fourier series expansion of the pulse train. Denoting this expansion as $K_1(t)$, the series becomes



TIME DOMAIN OUTPUT RESULTING FROM SCANNING THE IMAGE
BELOW NEGLECTING BLANKING



DIAGONAL BAR IMAGE

DIAGONAL BAR EXAMPLE

Figure 9

$$K_1(t) = \sum_{n=-\infty}^{\infty} K_1(n) e^{jn\omega_f t} \quad (24)$$

$$\text{Where } K_1(n) = \frac{1}{t_f} \int_0^{t_f} K_1(t) e^{-jn\omega_f t} dt$$

$$\text{And } \omega_f = 2\pi f_f$$

Thus carrying out the indicated integration for the pulse train in question, $K_1(n) = \tau e^{-jn\omega_f \tau} \frac{(\sin n\omega_f \tau/2)}{n\omega_f \tau/2}$ (25)

Thus the envelope of $K_1(t)$ is given by the familiar $\sin x/x$ distribution with the first zero occurring when $\omega = 1/\tau$.

However, the spectrum of $v(t)$ is given by a summation of ℓ such pulse trains or

$$v(t) = \sum_{i=0}^{\ell} K_i(t) \quad (26)$$

By substituting Equation 24 into Equation 26, the Fourier series representation of $v(t)$ becomes

$$V(t) = \sum_{i=0}^{\ell} \sum_{n=-\infty}^{\infty} K_i(n) e^{jn\omega_f t} \quad (27)$$

An inspection of Equation 27 reveals that the summing of these pulse trains affects only the amplitude of the components. Thus for some fixed n , say n_1 , it is necessary to sum all of the K_i' s from each train of pulses to find the amplitude of the component at n_1 . But for some fixed n , the amplitude of all the K_i 's is the same and the only difference in the K_i 's is the phase of the components.

This phase difference is caused by the fact that the beginning on one pulse train is delayed by one line scan period (plus Δt due to the slant of the line) from the preceding pulse train. Thus, the phaseshift θ as function of the time delay, t_d , between pulses is given by

$$\theta = 2\pi t_d f \quad (28)$$

Where f is the frequency of the component in question.

The time delay, t_d , between the first and second pulses is $t_l + \Delta t$; and between the first and third, it is twice this much or, in general for the i^{th} pulse, it is $i(t_l + \Delta t)$. The amplitude of the n_1 component, $A(n_1)$, may be now expressed as the sum of terms with identical amplitudes and phases given by Equation 28 or

$$A(n_1) = K_1(n_1) + K_2(n_1) e^{j2\pi t_d f} + K_3(n_1) e^{j4\pi t_d f} + \dots \\ + \dots + K_l(n_1) e^{j2\pi l t_d f}.$$

However, by recalling the $K_1(n_1) = K_2(n_1) = \dots = K_l(n_1)$ the expression reduces to

$$A(n_1) = K(n_1) \sum_{i=0}^l e^{j2\pi i T f} \quad (29)$$

$$\text{Where } T = t_l + \Delta t.$$

However, the series in Equation 29 may be put into closed form (10), and the results are

$$\sum_{i=0}^l e^{j2\pi i T f} = \frac{\sin \pi l T f}{\sin \pi T f} \quad (30)$$

Substitution of Equation 30 into Equation 29 yields an expression for $A(n_1)$.

$$A(n_1) = \left| K(n_1) \frac{\sin \pi \ell T f}{\sin \pi T f} \right| \quad (31)$$

Since Equation 31 is good for any fixed n , it may be substituted into Equation 27 to obtain the Fourier series representation of $v(t)$ as

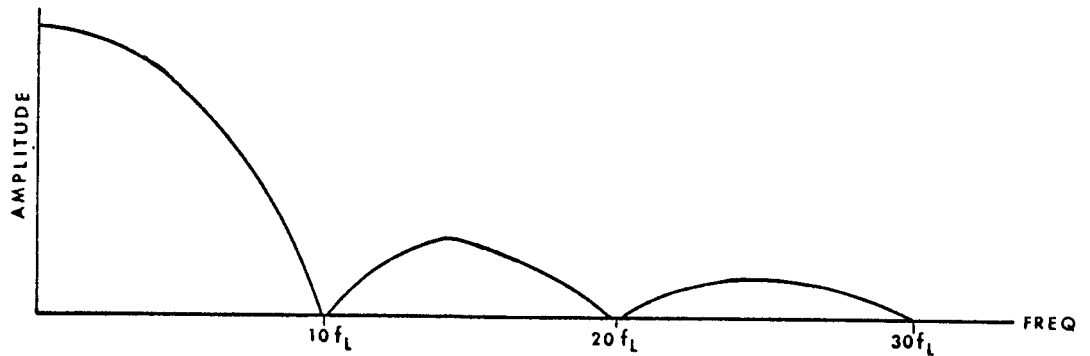
$$v(t) = \sum_{n=-\infty}^{\infty} \left| K(n) \frac{\sin \pi \ell T n f}{\sin \pi T n f} \right| e^{j n \omega_f t} \quad (32)$$

The envelope of the resulting $v(t)$ has been plotted in Figure 10 assuming a vertical line; i.e., $\Delta t = 0$. The effect of having the sum of pulse trains instead of only one pulse train is to modulate the envelope of $K(n)$ with

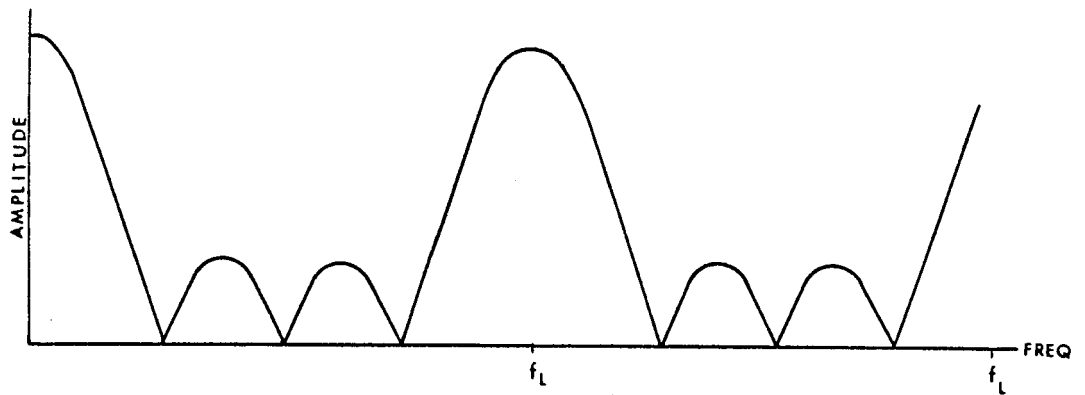
$$\frac{\sin \pi \ell T n f}{\sin \pi T n f}$$

The main effect of this modulation is to concentrate the energy in bands about the harmonics of the line frequency. Observe that this concentration is accomplished without consideration of the blanking frequency, and that when the pulse width is small, the effect of the blanking signal on the composite video spectrum is very minor by the arguments presented in the last section. Thus, in this case, the bandwidth necessary to transmit the composite video signal is determined by the $v(t)$ and, more specifically, by the $\sin x/x$ envelope of one of the pulses.

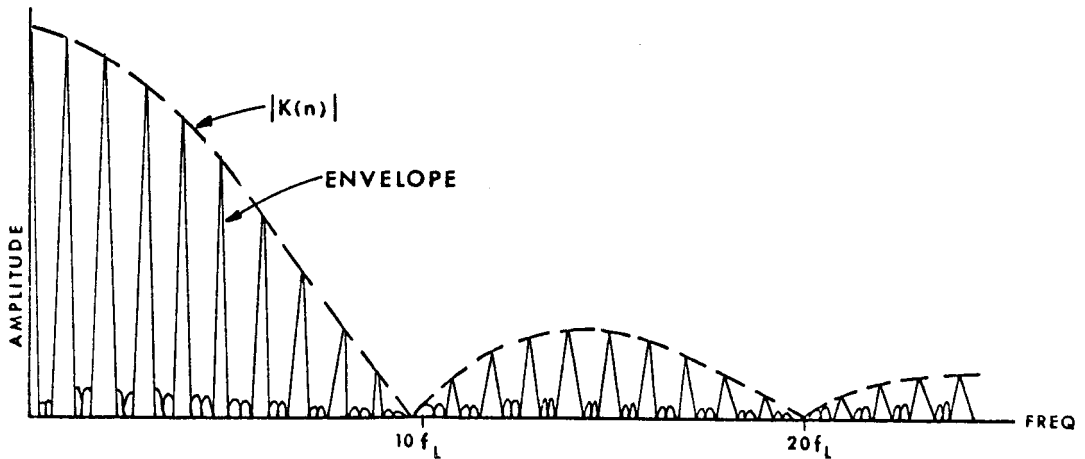
One last point of interest is what happens when Δt is not zero; i.e., when the line is rotated. Examination of the modulating function will reveal that it is periodic and has peaks located at $f = \frac{1}{T}$.



MAGNITUDE OF $K(n)$ FOR DIAGONAL BAR



AMPLITUDE OF $\left| \frac{\sin \pi L T N f}{\sin \pi T N f} \right|$ WITH $T = 1/f_L$



ENVELOPE OF THE VIDEO SPECTRUM OF THE DIAGONAL BAR SPECTRUM FOR DIAGONAL BAR

Figure 10

Therefore, if Δt is not zero, then the peaks of the spectrum envelope occur at $f = \frac{1}{t_\ell + \Delta t}$ and harmonics of f . Thus, for a Δt small, in comparison with t_ℓ , the first peak is very near the line frequency, but for the higher harmonics of f , the peak occurs farther away from the line frequency and thus the spectrum becomes more diffused in the higher proportions of the video range for non-vertical lines.

This effect is analogous to putting a band of frequencies into a frequency doubling circuit, and the output is a band of frequencies twice as wide. For example, if Δt is $.01t_\ell$, then the first peak occurs at $f = .99f_\ell$, but the 50th peak occurs at $f = 49.5f_\ell$ or half way between the forty-ninth and fiftieth harmonic of the line frequency.

Summary

In this chapter, a mathematical model for the composite video signal has been presented and the resulting spectrum for the composite video signal derived. Examples have been presented using this model, and the relationship between the blanking and video signal on the resulting composite video signal has been shown heuristically to be a function of the bandwidths of each signal taken separately. A first order approximation to the bandwidth necessary to transmit a given video signal, $v(t)$ has been shown and the factors affecting this bandwidth discussed. However, there has been no general method given for obtaining $v(t)$ which for complex program material, becomes quite difficult by the methods used in this chapter. This problem will be dealt with in Chapter IV.

One ray of encouragement concerning this model is that the results obtained for wide-band $v(t)$'s agree with those obtained by L.E. Franks using a random video model (9).

CHAPTER IV

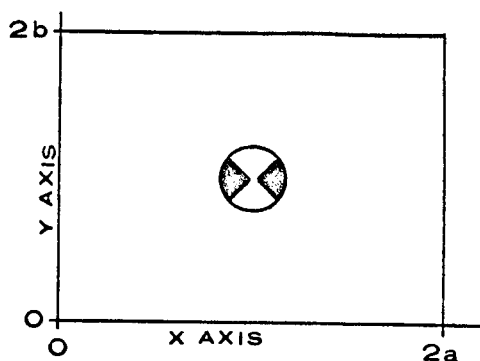
GENERAL METHOD FOR OBTAINING THE SPECTRUM OF THE VIDEO SIGNAL

General Discussion

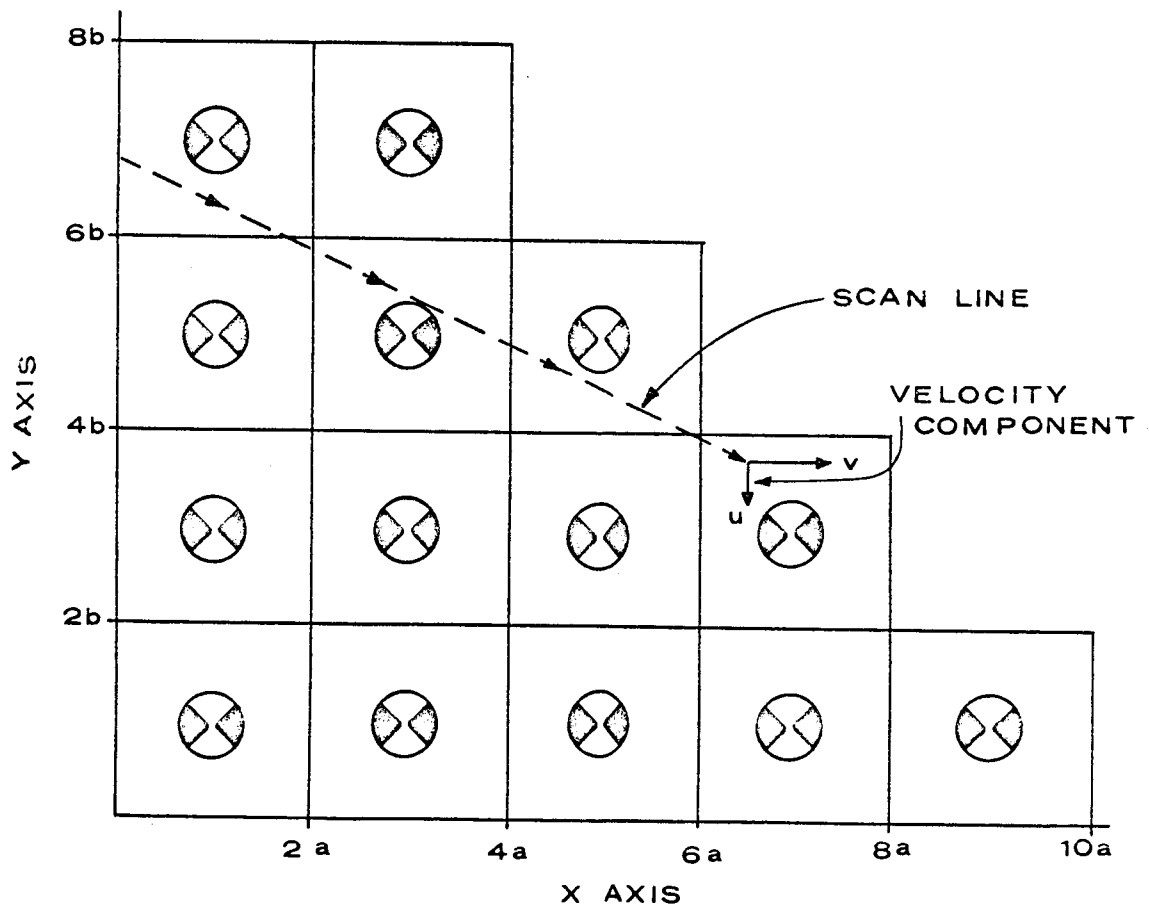
In Chapter III, a mathematical model of the composite video signal was presented, but in order to use this model, it is necessary to evaluate the function $v(t)$. This function may be obtained by performing the scanning process mentally and thus generating the video signal, as was done for the previous two examples. However, this process becomes very complicated for a picture of any complexity. Thus, it would be very advantageous to have a method for obtaining the spectrum of $v(t)$ directly from the image and thus avoid the step of transformation into the time domain. In this chapter, a method developed by P. Mertz and F. Gray for obtaining the spectrum of $v(t)$ directly will be presented, and a numerical technique for machine computation based on this method will be developed.

Harmonic Analysis of Scanned Optical Images

Figure 11 represents a typical image to be transmitted through a television system. If the brightness function over the surface is defined as $B(x,y)$, then along any fixed y , say y_1 , it is possible to expand $B(x,y_1)$ in a spatial Fourier series by assuming that the picture is periodic along x axis. This assumption does not degrade the results, since what is outside the interval from $x=0$ to $x=2a$ is not specified by the image in question: i.e., $B(x,y)$ may be defined in any manner which is useful outside of this interval.



TYPICAL IMAGE AND COORDINATE SYSTEM



PERIODIC STRUCTURE USED TO OBTAIN THE VIDEO SPECTRUM OF THE IMAGE ABOVE

TYPICAL IMAGE & COORDINATE SYSTEM USED

Figure 11

Thus, $B(x, y_1)$ may be expressed as

$$B(x, y_1) = \sum_{k=-\infty}^{\infty} A_k e^{j \frac{\pi k}{a} x}. \quad (33)$$

If y_1 is allowed to change to some other y , then the only effect on Equation 33 is to change the A_k 's. It follows that if $B(x, y)$ is allowed to become periodic in the y direction, also, that A_k may then be expanded into a Fourier series in y or that A_k becomes

$$A_k = \sum_{l=-\infty}^{\infty} C_{kl} e^{j \frac{\pi l}{b} y}. \quad (34)$$

Substitution of Equation 34 into Equation 33 yields a general expression for $B(x, y)$: i.e., $B(x, y)$ becomes

$$B(x, y) = \sum_{k=-\infty}^{\infty} \sum_{l=-\infty}^{\infty} C_{kl} e^{j \left(\frac{\pi k}{a} x + \frac{\pi l}{b} y \right)} \quad (35)$$

The effect of scanning such an image is to make both x and y functions of t . Then as x and y vary with time, a narrow strip is scanned across each of the pictures in the xy plane so that the total effect is to repeatedly scan this image and, therefore, to generate a $v(t)$ which corresponds to the video output produced by scanning a still image. (See Figure 11). Thus, $v(t)$ may be expressed as

$$v(t) = A_g \sum_{k=-\infty}^{\infty} \sum_{l=-\infty}^{\infty} C_{kl} e^{j \left(\frac{\pi k v}{a} + \frac{\pi l u}{b} \right) t} \quad (36)$$

Where $x = vt$

$y = ut$

A_g = conversion gain of the scanning device

v = velocity of the scanning device in the
x direction

u = velocity of the scanning device in the
y direction

By combining the $+k, +l$ components with the $-k, -l$ components and the $-k, +l$ components with the $+k, -l$ components, Equation 36 may be written as a cosine series.

$$v(t) = \sum_{k=0}^{\infty} \sum_{l=-\infty}^{\infty} A_{kl} \cos \left[\pi \left(\frac{vk}{a} + \frac{ul}{b} \right) t + \phi_{kl} \right] \quad (37)$$

Where $A_{kl} = 1/2 C_{kl} e^{j\phi_{kl}}$

$A_{-k, -l} = 1/2 C_{kl} e^{-j\phi_{kl}}$

A_g has been taken as one for convenience

However, Equation 37 may be further simplified by recalling $v/a = 2/t_\ell$ and $v/b = 2/t_f$ so that Equation 37 becomes

$$v(t) = \sum_{k=0}^{\infty} \sum_{l=-\infty}^{\infty} A_{kl} \cos [2\pi(f_\ell k + f_f l)t + \phi_{kl}] \quad (38)$$

Equation 38 represents the general form of the video output as a function of time and has the added advantage that it defines the spectrum of $v(t)$. Inspection of Equation 38 shows the components in the spectrum of $v(t)$ are the line frequency harmonics with sidebands about them consi-

sting of the frame frequencies. (See Figure 12). This should not be confused with the composite video frequency spectrum obtained in Chapter III, but rather this is the video spectrum before multiplication by the blanking signal.

The major advantage of expressing $v(t)$ in the form of Equation 38 is that the coefficients, A_{kl} , which determine the spectrum of $v(t)$ may be found directly from the image function, $B(x,y)$.

Using Equation 35, $B(x,y)$ may be reduced to a cosine expression using the same method as for $v(t)$. $B(x,y)$ then becomes,

$$B(x,y) = \sum_{k=0}^{\infty} \sum_{l=-\infty}^{\infty} A_{kl} \cos \left[\frac{\pi k}{a} x + \frac{\pi l}{b} y \right] t + \phi_{kl}.$$

However, this expression is expandable by use of trig identities into

$$B(x,y) = \sum_{k=0}^{\infty} \sum_{l=-\infty}^{\infty} a_{kl} \cos \left(\frac{\pi k}{a} x + \frac{\pi l}{b} y \right) + b_{kl} \sin \left(\frac{\pi k}{a} x + \frac{\pi l}{b} y \right) \quad (39)$$

$$\text{Where } a_{kl} = A_{kl} \cos \phi_{kl}$$

$$b_{kl} = A_{kl} \sin \phi_{kl}$$

It then follows by orthogonal relationships that

$$a_{pq} = \frac{1}{4ab} \int_0^{2a} \int_0^{2b} B(x,y) \cos \left(\frac{\pi p}{a} x + \frac{\pi q}{b} y \right) dx dy \quad (40)$$

and

$$b_{pq} = \frac{1}{4ab} \int_0^{2a} \int_0^{2b} B(x,y) \sin \left(\frac{\pi p}{a} x + \frac{\pi q}{b} y \right) dx dy. \quad (41)$$

Then since $A_{pq} = \sqrt{a_{pq}^2 + b_{pq}^2}$, the spectrum of $v(t)$ is completely defined by evaluation of the integrals of Equation 40 and Equation 41.

General Aspects of the Spectrum of $v(t)$

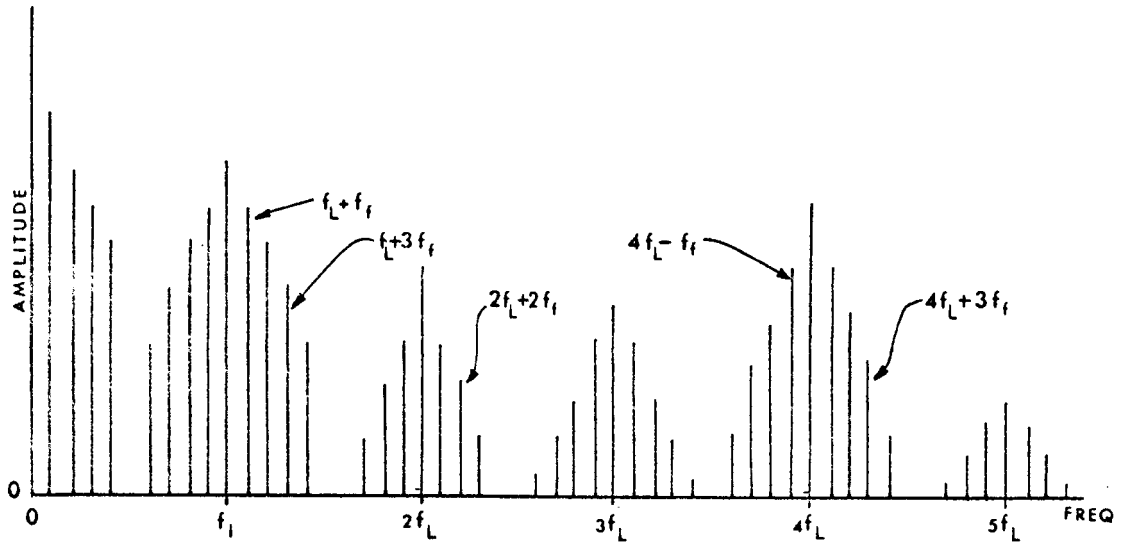
There are several points of interest concerning the video spectrum which are brought to light by this approach. The first of these is that the process of scanning transforms each of the spacial Fourier components of $B(x,y)$ into a component in the spectrum of $v(t)$. This transformation is made on a one to one basis and any nonlinearity in the scanning device which alters the amplitude of these components or generates new ones will produce distortion of the video signal.

Another item of interest is the effect of motion in the image. If the image is changing from one scan to another, then the effect this has on the Fourier series expansion of $B(x,y)$ is to make the coefficients, A_{kl} , functions of time. Since these coefficients are also the coefficients in the Fourier series expansion of $v(t)$, each component of $v(t)$ is of the form

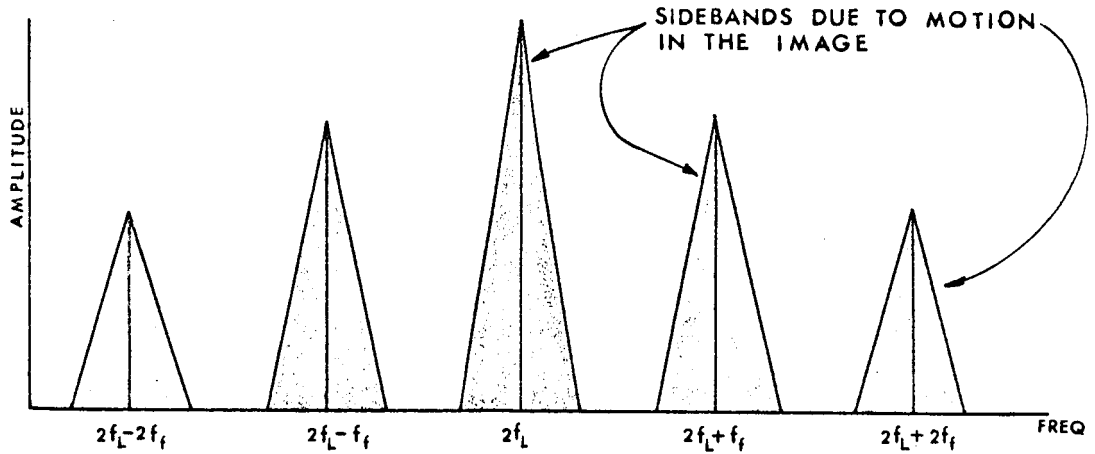
$$A(t) = A_{k_1 l_1}(t) \cos [(k_1 f_1 + l_1 f_f) 2\pi t + \phi_{k_1 l_1}]. \quad (42)$$

Where $A(t)$ is the amplitude of the $K_1 l_1$ component.

Inspection of Equation 42 reveals that it is an exact expression for a double sideband suppressed carrier signal. The spectrum of each component of $v(t)$ takes on sidebands with the maximum frequency of the sidebands equal to the maximum frequency of the motion in the image. Figure 12 is a blown-up portion of a part of such a spectrum of $v(t)$. Note that



TYPICAL AMPLITUDE SPECTRUM OF A VIDEO SIGNAL



DETAIL OF A TYPICAL REGION OF THE VIDEO SPECTRUM SHOWING THE EFFECT OF MOTION IN THE IMAGE

VIDEO SPECTRUMS

Figure 12

if the frequency of the motion is greater than $1/2$ the frame frequency, aliasing will result, causing a blurring effect in the received image.

Another point of interest is the effect of scanning with a finite aperture. Up to this point in the discussion, the aperture through which the scanning device viewed the image has been assumed to be a point. If it is not a point but rather a small area with its response dependent upon the location of the image point in the area, then these results must be modified. The effect of such an aperture is to smooth the time series representing $v(t)$ and thus to modify the spectrum much as a filter would. By extending this basic filter concept, Mertz and Gray (11) were able to show that a finite two dimensional aperture has the effect of a comb filter with its response peaks at the harmonics of the line frequency. Thus, the effect of a finite aperture on the spectrum is to further confine the components to bands of frequencies about the harmonics of the line frequency. (The convergence of the Fourier series expansion of $v(t)$ also has the effect of confining the energy to these bands in the spectrum.)

One precaution which must be observed in using this method is that $B(x,y)$ must truly be a function of both x and y . Otherwise, the integrals of Equations 40 and 41 are identically zero. However, this is not a fault of the theory, but rather a violation of one of its assumptions. Equation 34 tacitly assumes that the expansion of $B(x,y)$ for the two different y 's will change A_k ; however, if $B(x,y)$ is not a function of y , then this is no longer true and thus, the theory collapses. However, when this condition exists, the situation is easily rectified by expanding $B(x)$ or $B(y)$ in its corresponding one dimensional series.

Development of a Numerical Method for Approximating the Spectrum
of $v(t)$

It is desirable to have a numerical technique for approximating the spectrum of $v(t)$ in order to avoid evaluation of the integrals in Equation 40 and Equation 41. The reason for avoiding this integration is the difficulty of obtaining a mathematical expression for $B(x,y)$ when the image is normal program material. In order to obtain such an approximation, it is sufficient to make x and y discrete and then find coefficients of the double Fourier series such that the series exactly represents $B(x,y)$ at the discrete points in question. If x is allowed to take on $2N$ values and y is allowed to take on $2M$ values, then x and y become periodic in $2N$ and $2M$ respectively. Taking the new periods of x and y into account, Equation 30 may be rewritten in an approximated form as

$$B(x,y) = \sum_{k=0}^{N-1} \sum_{\ell=0}^{M-1} \left[a_{k\ell} \cos \left(\frac{\pi k}{N} x + \frac{\pi \ell}{M} y \right) + b_{k\ell} \sin \left(\frac{\pi k}{N} x + \frac{\pi \ell}{M} y \right) \right] \quad (43)$$

Where $b_{0,\ell} = b_{k,0} = 0$

The reasons for the limits on the summation will become clear as formulas for $a_{k\ell}$ and $b_{k\ell}$ are derived. The dropping of the negative values of ℓ is possible because $a_{k,\ell} = a_{k,-\ell}$ and $b_{k\ell} = b_{k,-\ell}$; i.e., the spectrum is symmetrical with respect to the line frequency harmonics.

Thus, the problem of expanding the Equation 43 to obtain the video spectrum resolves itself into the problem of obtaining $a_{k\ell}$ and $b_{k\ell}$ in a numerical form suitable for machine calculation. Before

proceeding to the deviation of these coefficients, it is helpful to prove three lemmas which are necessary in the actual derivation of the expressions for the coefficients.

Lemma I

$$\sum_{x=0}^{2N-1} \sum_{y=0}^{2M-1} \sum_{k=0}^{N-1} \sum_{l=0}^{M-1} b_{kl} \sin\left(\frac{\pi k}{N}x + \frac{\pi l}{M}y\right)$$

$$\cos\left(\frac{\pi p}{N}x + \frac{\pi q}{M}y\right) = 0$$

Proof:

$$S = \sum_x \sum_y \sum_k \sum_l b_{kl} \sin\left(\frac{\pi k}{N}x + \frac{\pi l}{M}y\right) \cos\left(\frac{\pi p}{N}x + \frac{\pi q}{M}y\right)$$

Expanding by trig. identities

$$S = \sum_x \sum_y \sum_k \sum_l b_{kl} \left(\sin\frac{\pi k}{N}x \cos\frac{\pi l}{M}y + \cos\frac{\pi k}{N}x \sin\frac{\pi l}{M}y \right) \\ \left(\cos\frac{\pi p}{N}x \sin\frac{\pi q}{M}y - \sin\frac{\pi p}{N}x \cos\frac{\pi q}{M}y \right)$$

Carrying out the indicated multiplication

$$S = \sum_x \sum_y \sum_k \sum_l b_{kl} \sin\frac{\pi k}{N}x \cos\frac{\pi l}{M}y \cos\frac{\pi p}{N}x \cos\frac{\pi q}{M}y - \\ \sum_x \sum_y \sum_k \sum_l b_{kl} \sin\frac{\pi k}{N}x \sin\frac{\pi p}{N}x \cos\frac{\pi l}{M}y \sin\frac{\pi q}{M}y + \\ \sum_x \sum_y \sum_k \sum_l b_{kl} \cos\frac{\pi k}{N}x \sin\frac{\pi l}{M}y \cos\frac{\pi p}{N}x \cos\frac{\pi q}{M}y -$$

$$\sum_x \sum_y \sum_k \sum_l b_{kl} \cos \frac{\pi k}{N} x \sin \frac{\pi l}{M} y \sin \frac{\pi p}{N} x \sin \frac{\pi q}{M} y$$

and by rearranging

$$S = \sum_{y=0}^{2M-1} \sum_{k=0}^{N-1} \sum_{l=0}^{M-1} b_{kl} \cos \frac{\pi l}{M} y \cos \frac{\pi q}{M} y \sum_{x=0}^{2N-1} \sin \frac{\pi k}{N} x \cos \frac{\pi p}{N} x -$$

$$\sum_{x=0}^{2N-1} \sum_{k=0}^{N-1} \sum_{l=0}^{M-1} b_{kl} \sin \frac{\pi k}{N} x \sin \frac{\pi p}{N} x \sum_{y=0}^{2M-1} \cos \frac{\pi l}{M} y \sin \frac{\pi q}{M} y +$$

$$\sum_{x=0}^{2N-1} \sum_{k=0}^{N-1} \sum_{l=0}^{M-1} b_{kl} \cos \frac{\pi k}{N} x \cos \frac{\pi p}{N} x \sum_{y=0}^{2M-1} \cos \frac{\pi q}{M} y \sin \frac{\pi l}{M} y -$$

$$\sum_{y=0}^{2M-1} \sum_{k=0}^{N-1} \sum_{l=0}^{M-1} b_{kl} \sin \frac{\pi l}{M} y \sin \frac{\pi q}{M} y \sum_{x=0}^{2N-1} \sin \frac{\pi p}{N} x \cos \frac{\pi k}{N} x$$

but it known that (12)

$$\sum_{z=0}^{2i-1} \sin \frac{\pi}{i} jz \cos \frac{\pi}{i} hz = 0 \quad (\text{A})$$

Thus applying this theorem to each of the single series above S becomes,

$$S = 0$$

QED

Lemma 2

$$\sum_{x=0}^{2N-1} \sum_{y=0}^{2M-1} \sum_{k=0}^{N-1} \sum_{l=0}^{M-1} a_{kl} \cos \left(\frac{\pi k}{N} x + \frac{\pi l}{M} y \right) \cos \left(\frac{\pi p}{N} x + \frac{\pi q}{M} y \right) =$$

$$2 a_{pq}^{MN} \quad \begin{array}{l} 0 < q < M-1 \\ 0 < p < N-1 \\ p \text{ and } q \text{ not both zero} \end{array}$$

Proof: Letting S be equal to the sum and expanding by use of trig

identities and separating the resultant series in the same manner as used in Lemma 1.

$$S = \sum_{k=0}^{N-1} \sum_{\ell=0}^{M-1} a_{k\ell} \sum_{x=0}^{2N-1} \cos \frac{\pi k}{N} x \cos \frac{\pi p}{N} x \sum_{y=0}^{2M-1} \cos \frac{\pi \ell}{M} y \cos \frac{\pi q}{M} y -$$

$$\sum_{k=0}^{N-1} \sum_{\ell=0}^{M-1} a_{k\ell} \sum_{x=0}^{2N-1} \cos \frac{\pi k}{N} x \sin \frac{\pi p}{N} x \sum_{y=0}^{2M-1} \cos \frac{\pi \ell}{M} y \sin \frac{\pi q}{M} y -$$

$$\sum_{k=0}^{N-1} \sum_{\ell=0}^{M-1} a_{k\ell} \sum_{x=0}^{2N-1} \cos \frac{\pi p}{N} x \sin \frac{\pi k}{N} x \sum_{y=0}^{2M-1} \cos \frac{\pi q}{M} y \sin \frac{\pi \ell}{M} y +$$

$$\sum_{k=0}^{N-1} \sum_{\ell=0}^{M-1} a_{k\ell} \sum_{x=0}^{2N-1} \sin \frac{\pi k}{N} x \sin \frac{\pi p}{N} x \sum_{y=0}^{2M-1} \sin \frac{\pi \ell}{M} y \sin \frac{\pi q}{M} y$$

Then by use of A from Lemma 1, the second and third series become zero and S reduces to,

$$S = \sum_{k=0}^{N-1} \sum_{\ell=1}^{M-1} a_{k\ell} \sum_{x=0}^{2N-1} \cos \frac{\pi k}{N} x \cos \frac{\pi p}{N} x \sum_{y=0}^{2M-1} \cos \frac{\pi \ell}{M} y \cos \frac{\pi q}{M} y +$$

$$\sum_{k=0}^{N-1} \sum_{\ell=0}^{M-1} a_{k\ell} \sum_{x=0}^{2N-1} \sin \frac{\pi k}{N} x \sin \frac{\pi p}{N} x \sum_{y=0}^{2M-1} \sin \frac{\pi \ell}{M} y \sin \frac{\pi q}{M} y.$$

But it is known that (12)

$$\sum_{z=0}^{2i-1} \sin \frac{\pi}{i} j z \sin \frac{\pi}{i} h z = 0 \quad \begin{array}{l} j \neq h \\ i \quad j = h \neq 0 \\ 0 \quad j \text{ or } h = 0. \end{array} \quad (B)$$

$$\sum_{z=0}^{2i-1} \cos \frac{\pi}{i} j z \cos \frac{\pi}{i} h z = 0 \quad \begin{array}{l} j \neq h \\ i \quad j = h \neq 0, N, 2N, \dots \\ 2i \quad j = h = 0, N, 2N, \dots \end{array} \quad (C)$$

By applying B and C to the sine and cosine series respectively, S reduces to

$$S = a_{pq}^{NM} + a_{pq}^{NM} = 2a_{pq}^{NM}, \quad \begin{array}{l} 0 < q \leq M-1 \\ 0 < p \leq N-1 \end{array}$$

$$S = 2a_{pq}^{MN} + 0 = 2a_{pq}^{NM}, \quad \begin{array}{l} 0 < q \leq M-1 \\ 0 = p \quad \text{OR} \quad 0 = q \\ 0 < p \leq N-1 \end{array}$$

Therefore

$$S = 2a_{pq}^{MN}, \quad \begin{array}{l} 0 < q \leq M-1 \\ 0 < p \leq N-1 \\ q = p \neq 0 \end{array}$$

QED

Lemma 3

$$\sum_{x=0}^{2N-1} \sum_{y=0}^{2M-1} \sum_{k=0}^{N-1} \sum_{l=0}^{M-1} b_{kl} \sin \left(\frac{\pi k}{N} x + \frac{\pi l}{M} y \right) \sin \left(\frac{\pi p}{N} x + \frac{\pi q}{M} y \right) =$$

$$2M N b_{pq} \quad \begin{array}{l} 0 < p \leq N-1 \\ 0 < q \leq M-1 \end{array}$$

Proof : Once again letting S be the sum and expanding by trig identities and separating the series.

$$\begin{aligned}
S &= \sum_{k=0}^{N-1} \sum_{l=0}^{M-1} b_{kl} \sum_{x=0}^{2N-1} \sin \frac{\pi p}{N} x \sin \frac{\pi k}{N} x \sum_{y=0}^{2M-1} \cos \frac{\pi l}{M} y \cos \frac{\pi q}{M} y + \\
&\sum_{k=0}^{N-1} \sum_{l=0}^{M-1} b_{kl} \sum_{x=0}^{2N-1} \sin \frac{\pi k}{N} x \cos \frac{\pi p}{N} x \sum_{y=0}^{2M-1} \cos \frac{\pi l}{M} y \sin \frac{\pi q}{M} y + \\
&\sum_{k=0}^{N-1} \sum_{l=0}^{M-1} b_{kl} \sum_{x=0}^{2N-1} \cos \frac{\pi k}{N} x \sin \frac{\pi p}{N} x \sum_{y=0}^{2M-1} \sin \frac{\pi l}{M} y \cos \frac{\pi q}{M} y + \\
&\sum_{k=0}^{N-1} \sum_{l=0}^{M-1} b_{kl} \sum_{x=0}^{2N-1} \cos \frac{\pi k}{N} x \cos \frac{\pi p}{N} x \sum_{y=0}^{2M-1} \sin \frac{\pi l}{M} y \sin \frac{\pi q}{M} y
\end{aligned}$$

By use of A from Lemma 1, the second and third series are zero, and S reduces to

$$\begin{aligned}
S &= \sum_{k=0}^{N-1} \sum_{l=0}^{M-1} b_{kl} \sum_{x=0}^{2N-1} \sin \frac{\pi p}{N} x \sin \frac{\pi k}{N} x \sum_{y=0}^{2M-1} \cos \frac{\pi l}{M} y \cos \frac{\pi q}{M} y + \\
&\sum_{k=0}^{N-1} \sum_{l=0}^{M-1} b_{kl} \sum_{x=0}^{2N-1} \cos \frac{\pi k}{N} x \cos \frac{\pi p}{N} x \sum_{y=0}^{2M-1} \sin \frac{\pi l}{M} y \sin \frac{\pi q}{M} y
\end{aligned}$$

Then by use of B and C from Lemma 2

$$S = b_{pq} N M + b_{pq} N M = 2M N b_{pq} \quad \begin{array}{l} 0 < p \leq N-1 \\ 0 < q \leq M-1 \end{array}$$

$$S = 0 + 0 = 0 \quad \text{Either } p \text{ or } q \text{ zero}$$

It is now possible to derive expressions for a_{pq} and b_{pq} as functions of $B(x,y)$. Multiplying both sides of Equation 43 by $\cos(\frac{\pi p}{N}x + \frac{\pi q}{M}y)$ and summing over x and y yields

$$\sum_{x=0}^{2N-1} \sum_{y=0}^{2M-1} B(x,y) \cos\left(\frac{\pi p}{N}x + \frac{\pi q}{M}y\right) = \sum_x \sum_y \sum_k \sum_l a_{k\ell} \cos\left(\frac{\pi k}{N}x + \frac{\pi \ell}{M}y\right) \cos\left(\frac{\pi p}{N}x + \frac{\pi q}{M}y\right) + \sum_x \sum_y \sum_k \sum_l b_{k\ell} \sin\left(\frac{\pi k}{N}x + \frac{\pi \ell}{M}y\right) \cos\left(\frac{\pi p}{N}x + \frac{\pi q}{M}y\right)$$

$$\left(\frac{\pi p}{N}x + \frac{\pi q}{M}y\right) \cos\left(\frac{\pi p}{N}x + \frac{\pi q}{M}y\right) + \sum_x \sum_y \sum_k \sum_l b_{k\ell} \sin\left(\frac{\pi k}{N}x + \frac{\pi \ell}{M}y\right) \cos\left(\frac{\pi p}{N}x + \frac{\pi q}{M}y\right)$$

$$\left(\frac{\pi p}{N}x + \frac{\pi q}{M}y\right). \quad (44)$$

Applying Lemma 2 to the first sum on the right-hand side of Equation 44 and Lemma 1 to the second sum of Equation 44 reduces to

$$\sum_{x=0}^{2N-1} \sum_{y=0}^{2M-1} B(x,y) \cos\left(\frac{\pi p}{N}x + \frac{\pi q}{M}y\right) = 2MN a_{pq} \quad (45)$$

By rearranging Equation 45, the desired expression for a_{pq} is obtained as

$$a_{pq} = \frac{1}{2NM} \sum_{x=0}^{2N-1} \sum_{y=0}^{2M-1} B(x,y) \cos\left(\frac{\pi p}{N}x + \frac{\pi q}{M}y\right) \quad \begin{array}{l} 0 < p \leq N-1 \\ 0 < q \leq M-1 \\ p=q \neq 0 \end{array} \quad (46)$$

Similarly, multiplying Equation 43 through by $\sin(\frac{\pi p}{N}x + \frac{\pi q}{M}y)$

and summing over x and y , the expression for b_{pq} is seen to be

$$b_{pq} = \frac{1}{2NM} \sum_{x=0}^{2N-1} \sum_{y=0}^{2M-1} B(x,y) \cos \left(\frac{\pi p}{N} x + \frac{\pi q}{M} y \right) \quad \begin{array}{l} 0 < p \leq N-1 \\ 0 < q \leq M-1 \end{array} \quad (47)$$

Equations 46 and 47 are an approximation of the amplitude and phase spectrum of $v(t)$ according to Equation 43. Also Equations 46 and 47 are in a form which may be used for machine computation, since their evaluation requires no more than arithmetical operations.

Description of the Computer Program to Find the Spectrum of $v(t)$.

In order to use Equations 46 and 47 for machine computation, the brightness function $B(x,y)$ must be specified at $4MN$ points equally spaced over the image. In the program used on this project, this was done by forming B into a matrix and storing this matrix on tape. The values of M and N were taken as 150 each, thus yielding 90,000 data points over the image. These points are then read off the tape, and Equations 46 and 47 evaluated to give a_{pq} and b_{pq} . Since the amplitude spectrum is of primary interest the amplitude, $A_{pq} =$

$\sqrt{a_{pq}^2 + b_{pq}^2}$, is calculated and this is the result plotted in all the following spectrums. A copy of this program, as well as an example of the ones used to generate the B matrix, may be found in Appendix I.

The first image which was selected for analysis was a white

circle and a black background. This image was chosen for two reasons. The first was that it represents typical program material for the Apollo television system: i.e., such an image would be seen by astronauts as they approach the moon in their Apollo space capsule. Secondly, an exact analytical result for this image was given by Mertz and Gray in 1934 (11): and, therefore, it is a good one on which to try the program. Figure 13 is a plot of the video spectrum for such an image, and Table III is a comparison of the computer results with the previously mentioned analytical expression.

Another example for which analytical results are available is the diagonal bar presented in Chapter III. Therefore, as a second check on the computer algorithm, this spectrum was investigated. The spectrum of the white bar placed at an angle of 45° with the x axis was analysed using the computer routine. The results are presented in Figures 14, 15, & 16. Figure 14 is the spectrum of the line frequency harmonics and represents the over-all course spectrum. Observe that the envelope is very nearly the $\sin x/x$ distribution of a single pulse produced by the scanning process as was predicted in Chapter III. Figures 15 and 16 are blown-up versions of Figure 14, showing the fine detail of the spectrum--- both the low and the high frequency regions. The actual numbers are representative of the Apollo (mode 1) system. Observe that the spectrum is more diffused from the line frequency harmonics in the upper frequency regions, as was predicted for a non-vertical line in Chapter III.

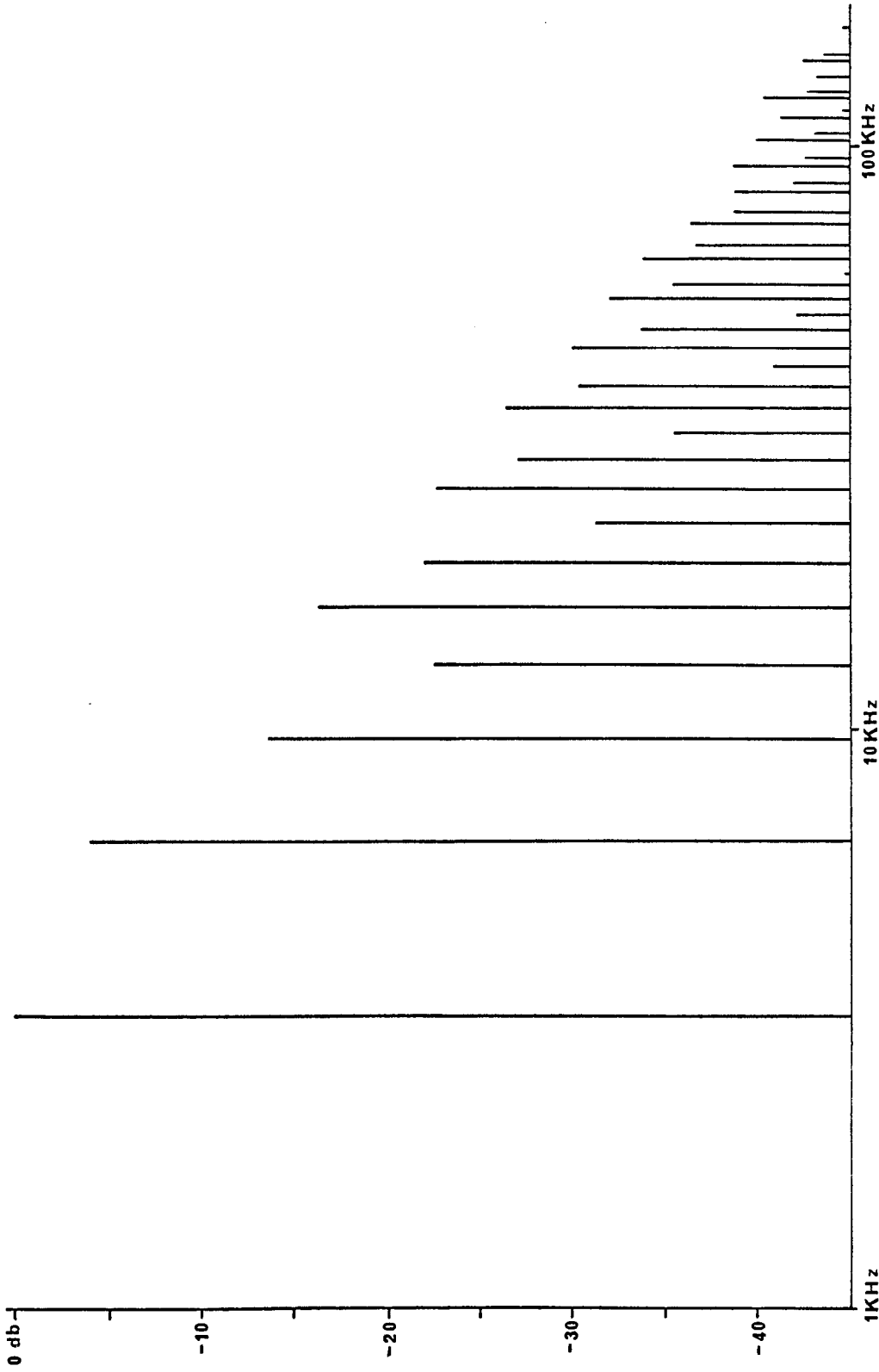
TABLE III

P	Q	*ACTUAL FREQUENCY IN Hz	CALCULATED AMPLITUDE	# MERTZ AND GRAY'S DIFFERENCE AMPLITUDE
1	0	3200	.152	.153 .001
1	1	3210	.131	.130 .001
1	2	3220	.079	.079 .000
1	3	3230	.023	.023 .000
1	4	3240	.014	.014 .000
2	0	6400	.094	.095 .001
2	1	6410	.079	.079 .000
2	2	6420	.042	.040 .002
2	3	6430	.0023	.0024 .0001
2	4	6440	.020	.021 .001
3	0	9600	.032	.032 .00
3	1	9610	.023	.023 .00
3	2	9620	.0023	.0024 .001
3	3	9630	.017	.017 .000
3	4	9640	.023	.023 .000
4	0	12800	.011	.012 .001
4	1	12810	.014	.014 .000
4	2	12820	.021	.021 .000
4	3	12830	.023	.023 .000
4	4	12840	.0169	.0168 .0001
5	0	16000	.023	.023 .000
6	0	19600	.0121	.0126 .0005
7	0	22800	.0041	.0047 .0006
8	0	26000	.0118	.0113 .0005
9	0	29200	.0065	.0061 .0004
10	0	32400	.0025	.0027 .0002
11	0	35600	.0072	.0071 .0001
12	0	38800	.0046	.0042 .0004
13	0	42000	.0014	.0019 .0005
14	0	45200	.0048	.0049 .0001

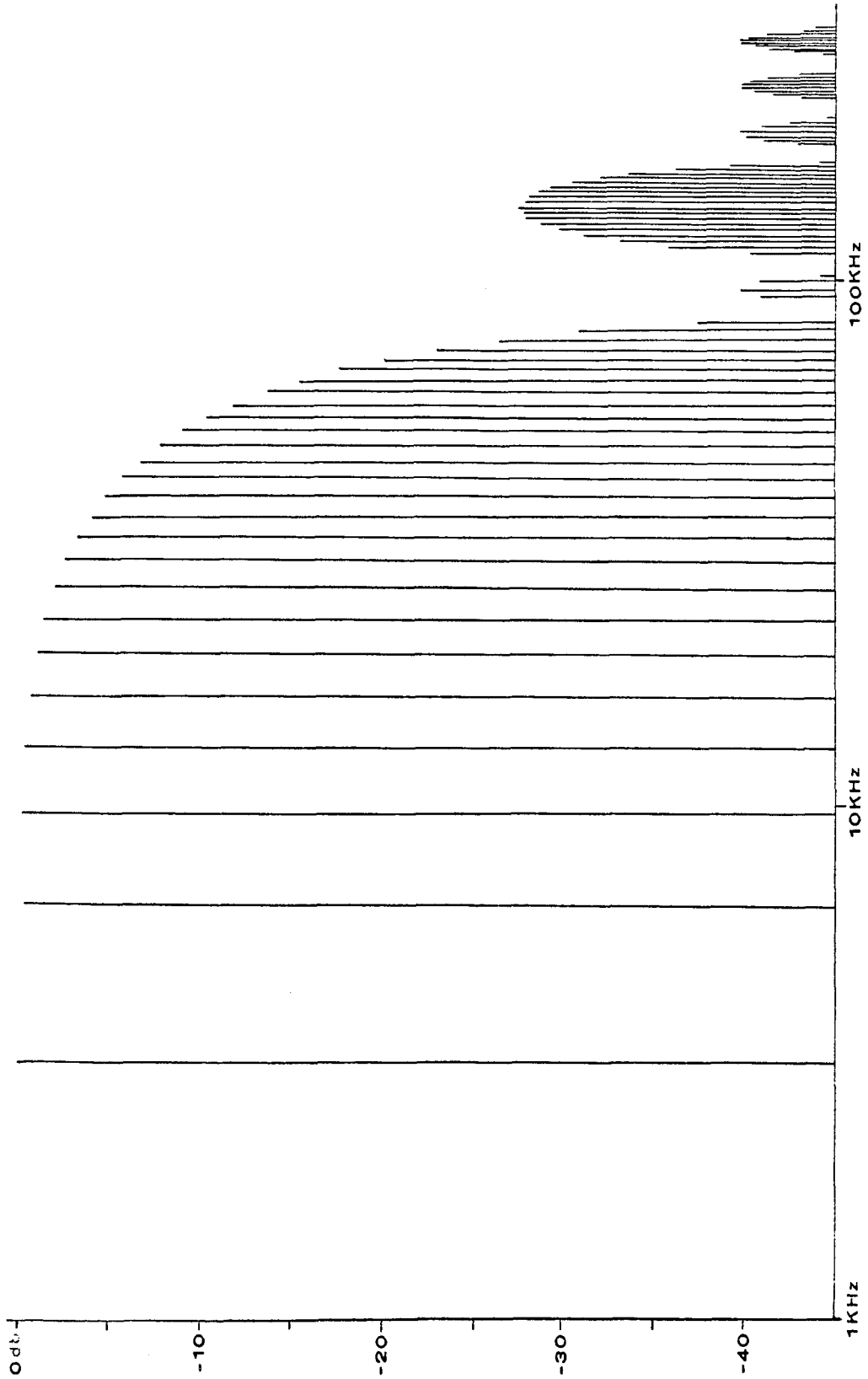
* Frequency Calculation based on Apollo mode 1 scanning parameters.

$$\#A_{pq} = \frac{R}{2ab} \left[\frac{1}{\left(\frac{P}{2a}\right)^2 + \left(\frac{Q}{2b}\right)^2} \right]^{1/2} J_1 \left[2\pi R \sqrt{\left(\frac{P}{2a}\right)^2 + \left(\frac{Q}{2b}\right)^2} \right]$$

Where a = length of picture
b = height of picture
R = radius of circle
 J_1 = order bessel function

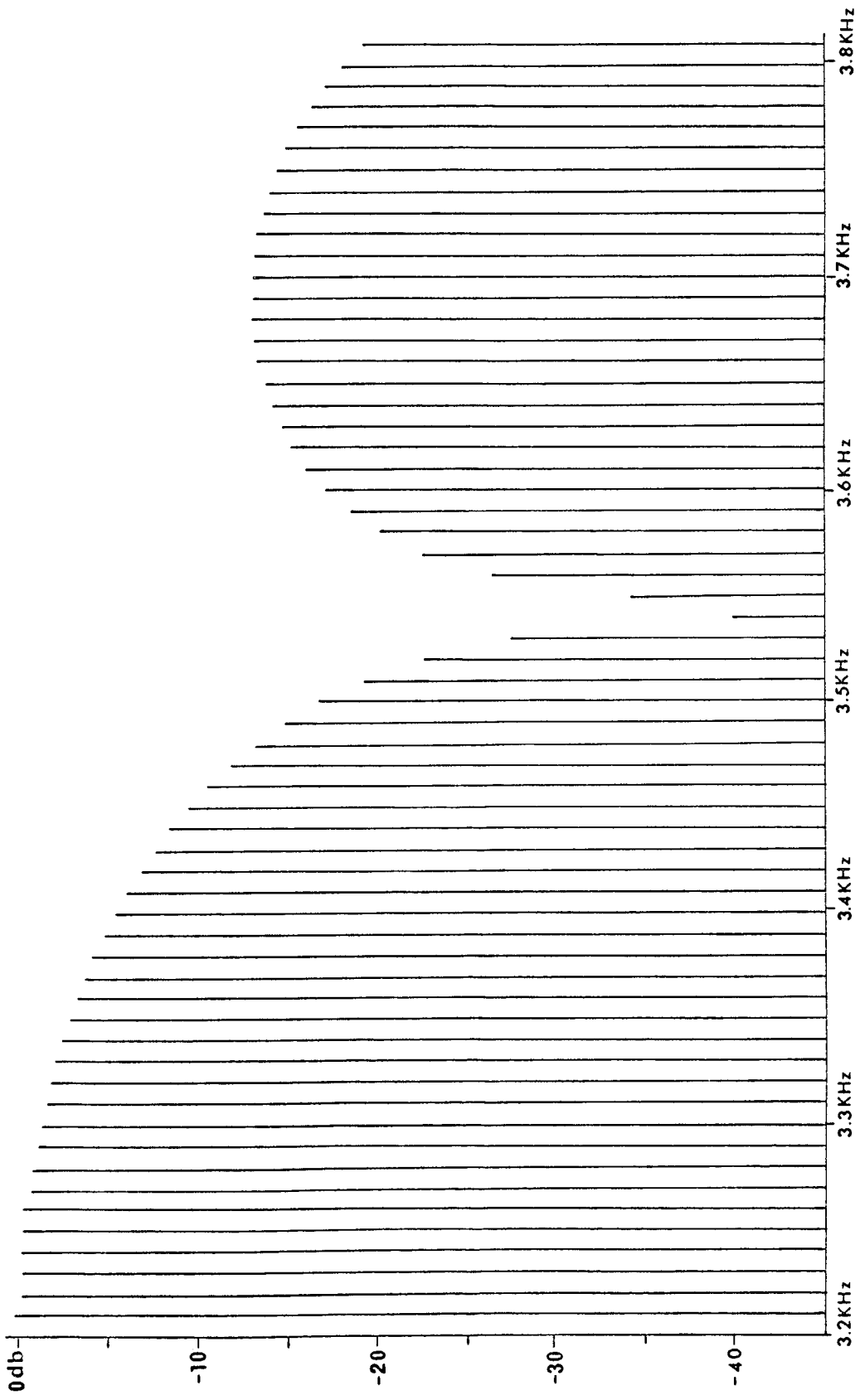


**SPECTRUM FOR WHITE CIRCLE OF
RADIUS 1/6 A ON A BLACK BACKGROUND**
Figure 13



SPECTRUM FOR DIAGONAL BAR TEST PATTERN

Figure 14



DETAIL OF DIAGONAL BAR
SPECTRUM IN LOW FREQUENCY REGION
Figure 15



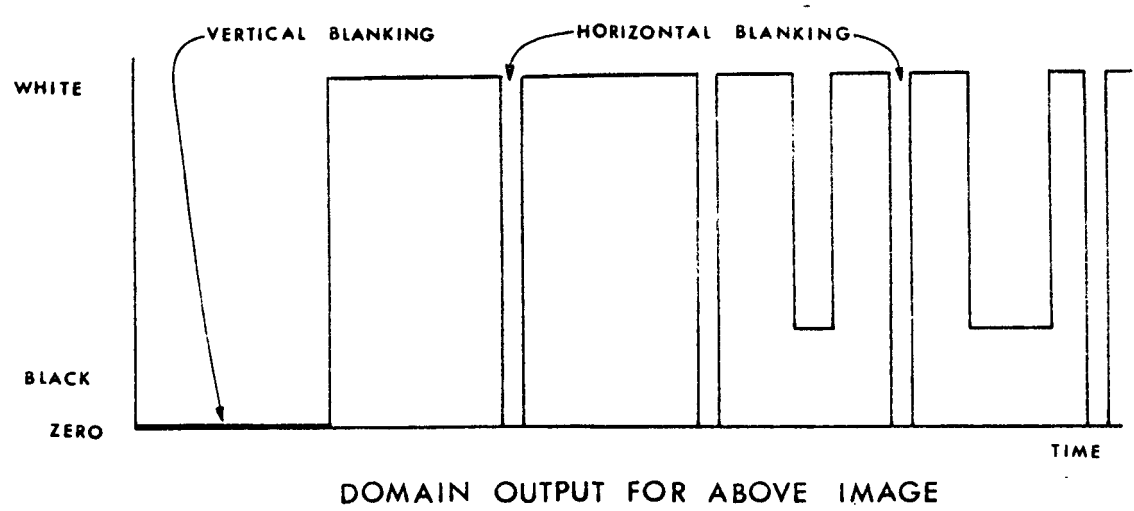
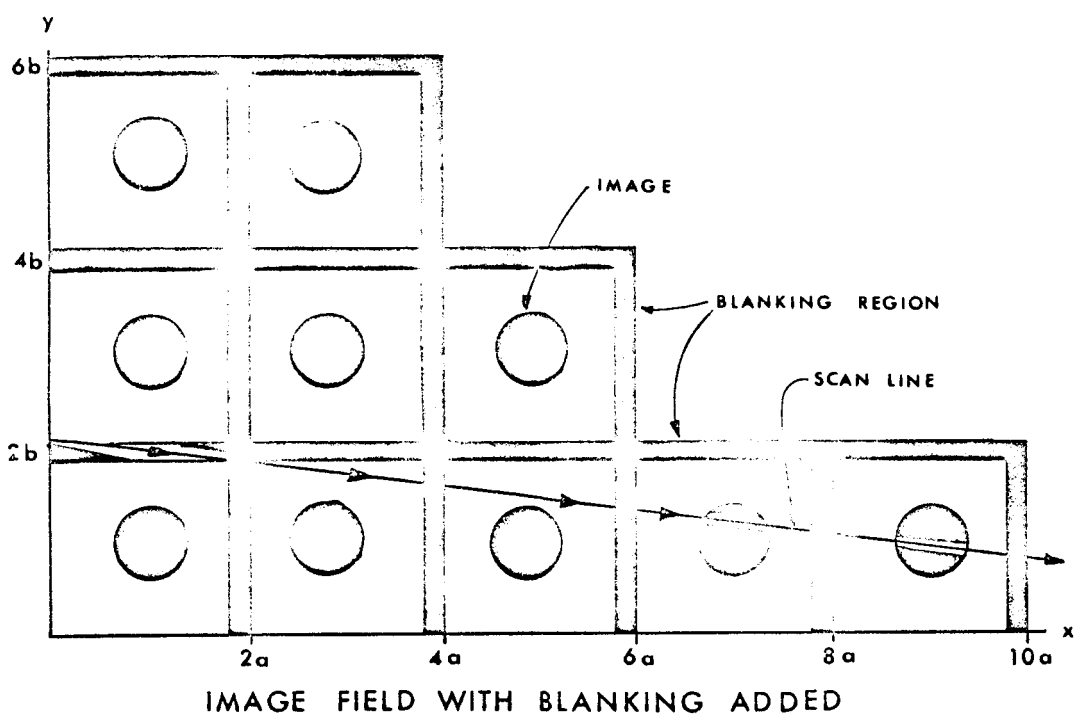
DETAIL OF DIAGONAL BAR
SPECTRUM IN HIGH FREQUENCY REGION
Figure 16

Extension of Computer Model to the Composite Video Spectrum

Up to this point in this chapter, the spectrum under consideration has been the spectrum of the video signal only ; i.e., without blanking and synchronization. Since in Chapter III the synchronization was shown to be an additive term resulting from a one dimensional series, neglecting this term represents a straight forward correction.

However, neglecting the blanking signals is a much more difficult item to correct, since the blanking functions are multiplying $v(t)$. Thus, if the model is to be of any real use, the blanking signals must be accounted for. With the computer algorithm already developed, the simplest method of adding the blanking is to put it into $B(x,y)$. This may be accomplished by placing a strip of zero brightness along the top of the image to represent vertical blanking and by placing a strip of zero brightness along the right hand edge to represent horizontal blanking. This argument is illustrated in Figure 17 and the resulting $v'(t)$ is sketched.

With this simple extension, the computer algorithm presented in the last section yields the composite video spectrum generated by transmitting any monochrome image. In the examples close observation will reveal that the nulls in the calculated spectrums are slightly shifted from those measured by NASA. The reason for this is the different ratios of the T/t_ℓ . NASA's ratio was .0965 while the best approximation to this which can be made using the previously mentioned 300 by 300 grid is .100.



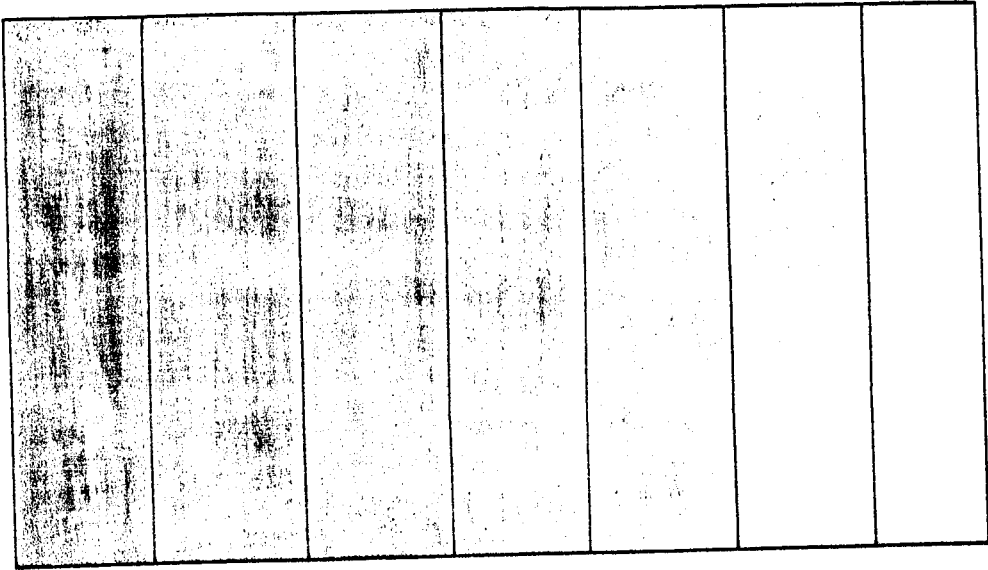
COMPOSITE VIDEO WAVEFORM

Figure 17

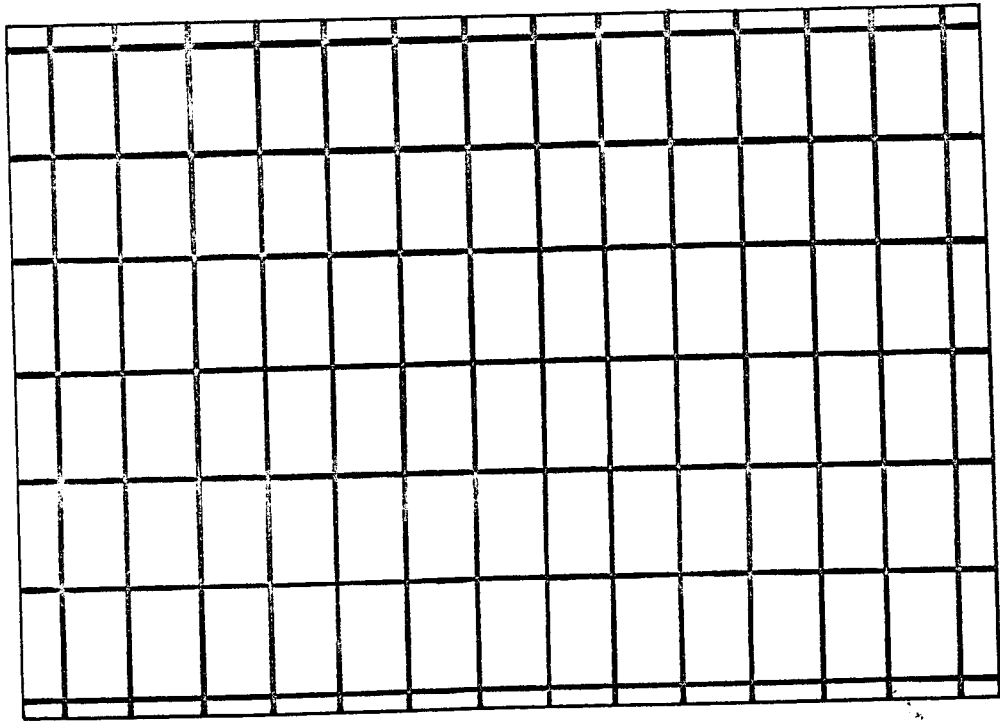
Composite Video Spectrums of Some Standard Test Patterns

With the model extended to the composite video spectrum, it is now feasible to determine spectrums of standard television test patterns. The ones selected for this study are representative of those used by NASA engineers for testing the Apollo system.

Knowing the theoretical spectrum of standard test patterns is important to television engineers for two reasons -- one being to insure the test pattern is actually testing the parameter of the system which it is designed to test, and secondly, to compare with experimental test data to evaluate system performance. Two patterns have been selected for this work to demonstrate the use of the model. They are the grate and gray scale patterns. These are shown in Figure 18. The contrast ratio in all cases is 100, and the plots of the spectrum are made using mode 1 Apollo scan parameters. The composite video spectrum produced by the grate pattern has been plotted in Figure 19. Figure 20 is a reproduction of the spectrum as measured by NASA test engineers. The agreement is seen to be quite good in general, with the major difference being in the large peak at 50 KHz which the computer algorithm predicted but NASA did not measure. However, the peaks at 100 KHz, 150 KHz, 200 KHz, and up do agree. The fact that NASA did measure a peak at 100 KHz and at intervals of 50 KHz thereafter indicates that these peaks are being generated by a 50 KHz fundamental and its harmonics. Thus, it would seem that the algorithm is correct and the lack of this large 50 KHz peak may represent an oversight in the measured spectrum.



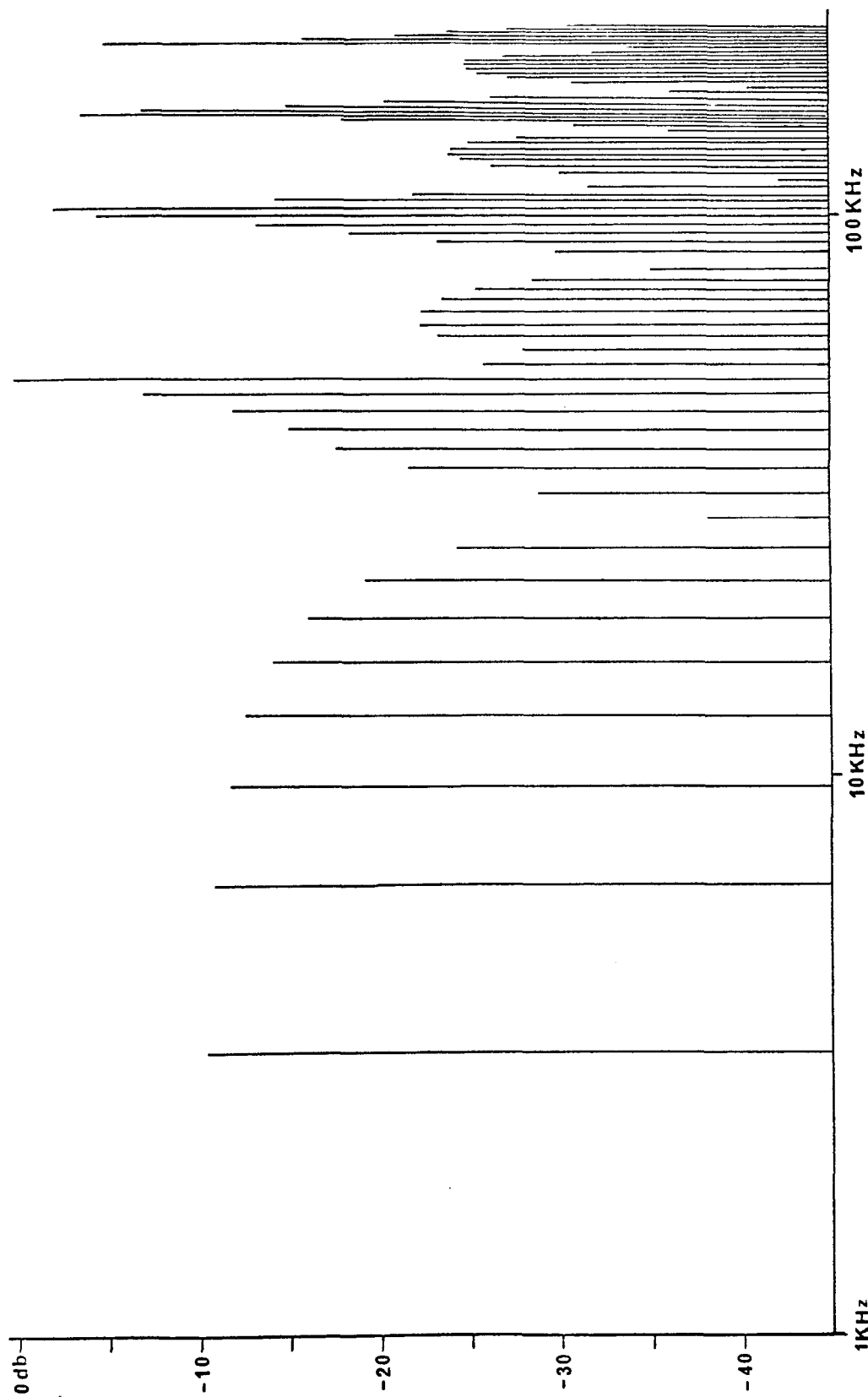
GRAY SCALE PATTERN



GRATE PATTERN

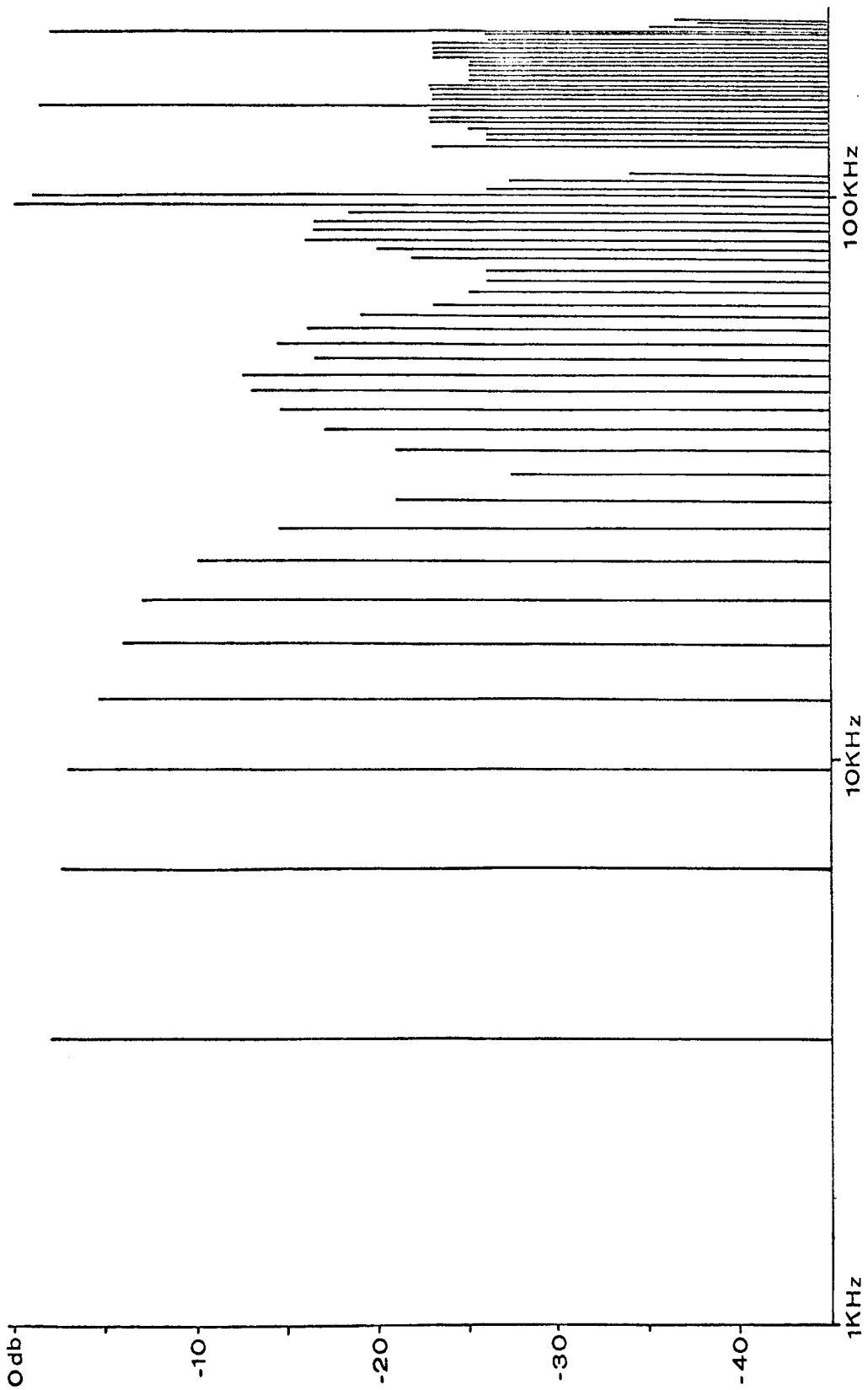
NASA TEST PATTERN

Figure 18



CALCULATED SPECTRUM FOR GRATE TEST PATTERN

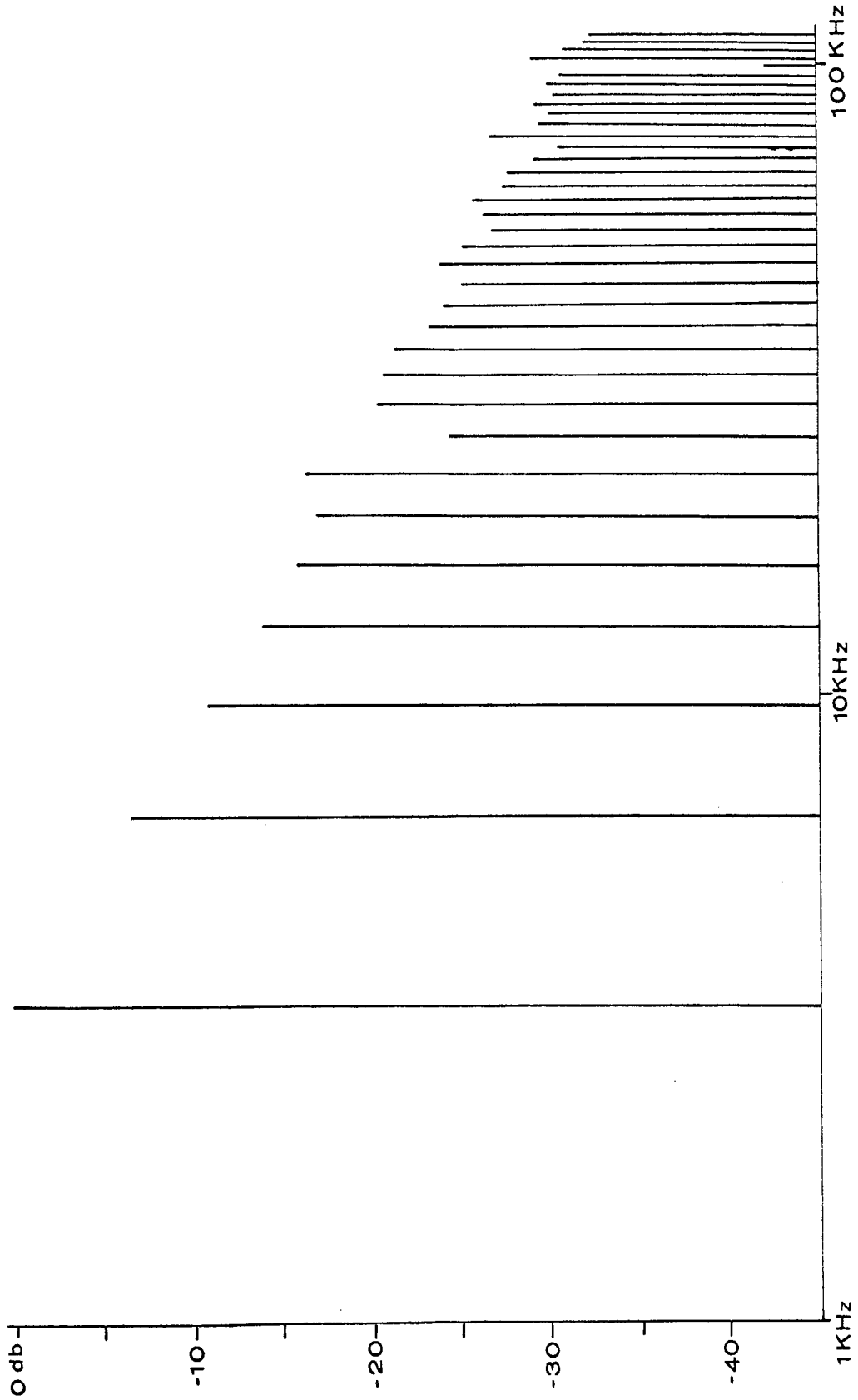
Figure 19



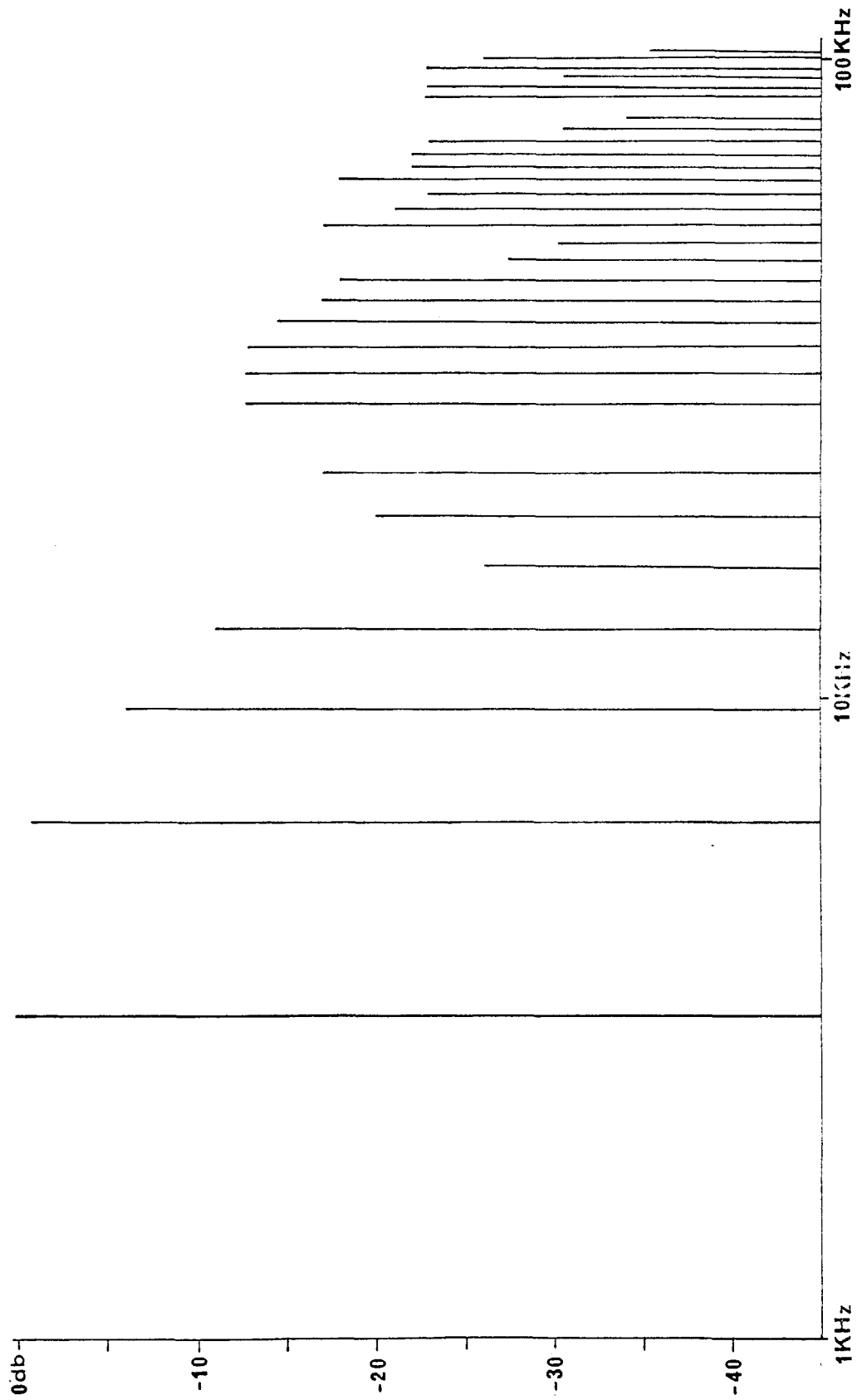
MEASURED SPECTRUM FOR GRATE TEST PATTERN
Figure 20

An interesting phenomenon was observed in calculating this spectrum. The contrast ratio first used was infinite, then changed to 1000, and finally changed to 100. As this ratio was decreased, the peaks of the spectrum were lower and the level of the valleys raised. This phenomenon apparently has not been observed by other workers in this area and needs experimental verification to prove or disprove that the contrast ratio has an effect on the composite video spectrum.

The second test pattern investigated was the gray scale or step pattern. The computer results are presented in Figure 21, and the spectrum as measured by NASA is shown in Figure 22. The general shape of these spectrums is the same, but the level of the peaks measured by NASA was much higher (approximately 5 to 12 db.) than those predicted by the computer results. This discrepancy is due to the difficulty in matching the levels of the various areas. As an example, Figure 23 is the same gray scale spectrum with a logmatic variation of brightness levels instead of the linear variation used in obtaining Figure 21. It can be seen by comparing the two that the logmatic variation of brightness levels produces a spectrum with lower peaks and higher valleys than the linear. Thus, for the actual variations used by NASA, the spectrum which they show may be entirely correct, but until those variations in brightness levels can be matched exactly, it is difficult to make any positive statement about the quality of these comparisons.

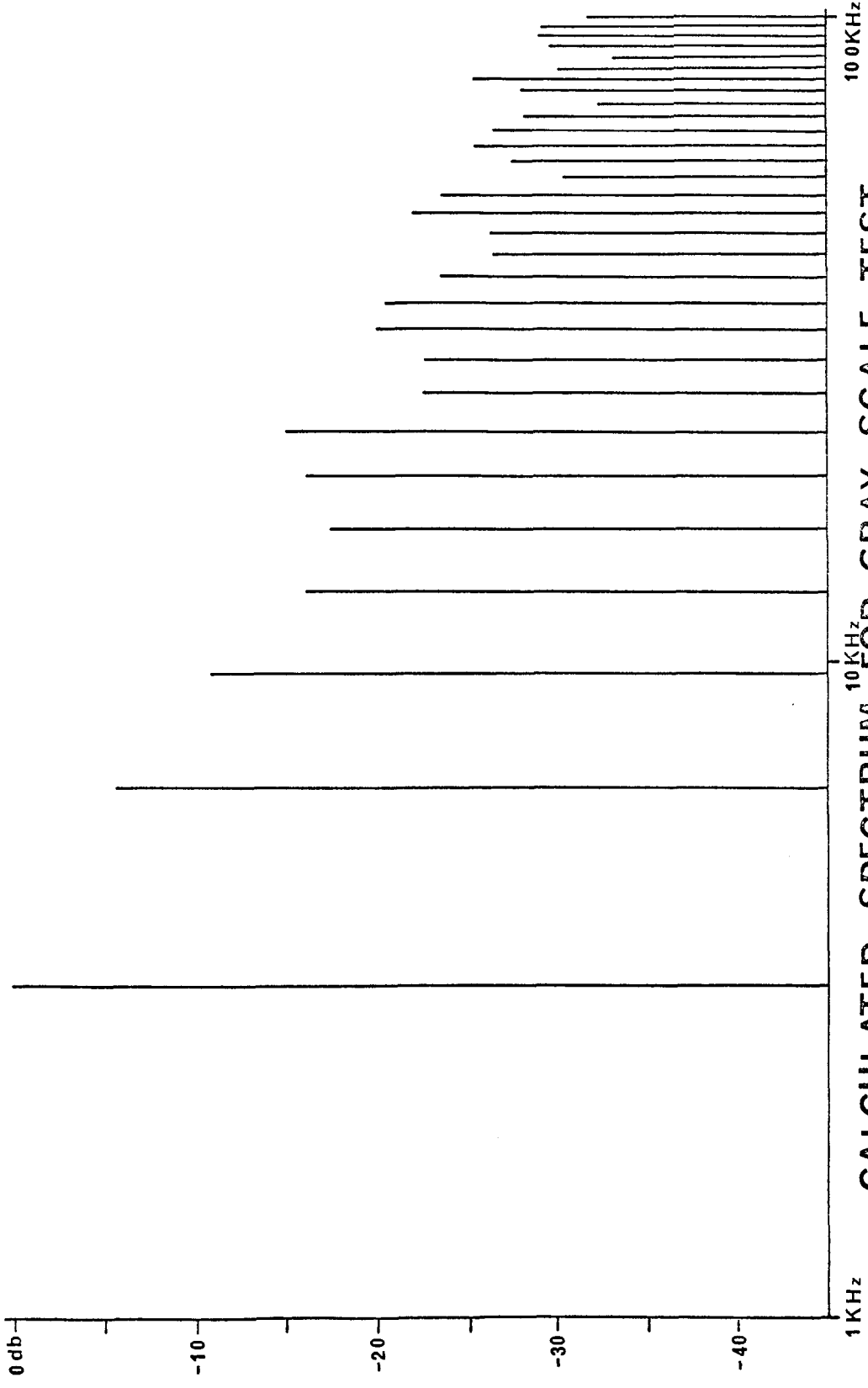


CALCULATED SPECTRUM FOR GRAY SCALE TEST
PATTERN WITH LINEAR BRIGHTNESS VARIATIONS
Figure 21



MEASURED SPECTRUM FOR GRAY SCALE TEST PATTERN

Figure 22



**CALCULATED SPECTRUM^{10 KHz} FOR GRAY SCALE TEST
PATTERN WITH LOGMATIC VARIATIONS IN BRIGHTNESS**

Figure 23

CHAPTER V

CONCLUSION

A mathematical model for a deterministic composite video signal has been presented and the resulting spectrum examined. The most difficult problem involved in using the model was obtaining the spectrum of the scanned video signal. This problem was solved by applying the methods of numerical analysis to the theory of scanning developed by Mertz and Gray and extending this theory to include blanking. The resulting computer program will obtain the composite video spectrum resulting from scanning any general image.

Obtaining the spectrum of the composite video signal was only half of the problem, however. The related problem of specifying the necessary bandwidth for a television system was discussed. The conclusions concerning bandwidth which may be drawn are twofold. First, if the program material which the television system must transmit is known, then the methods of this work may be applied to this material and the resulting spectrums will determine the necessary system bandwidth. The bandwidth determined in this manner will be a much better approximation than any of the methods presented in Chapter II. For example, if the only image to be transmitted is the half black and half white test pattern examined in Chapter III, then the necessary system bandwidth would be on the order 100 Kz. (Assuming Apollo mode 1 scan parameters). This is approximately one-fourth of the bandwidth predicted by any of the methods in Chapter II. However, if the only specification concerning the bandwidth available is the maximum

horizontal resolution, then the standard methods presented in Chapter II yield good estimations of the maximum bandwidth. Even in this case, it is feasible to use the methods of this work on probable images and let the results serve as a check on the standard methods.

An extension of this work to random video processes would relieve the burden of knowing the exact images to be transmitted. L. E. Franks of Bell Telephone Laboratories has recently published a paper in this area, but more work is needed to obtain reliable estimates of necessary bandwidth under actual operation conditions.

Another area of current interest to which this work may be applied is obtaining an estimate of the bandwidth resulting from frequency modulating a carrier with a composite video signal. This is of special interest in connection with the Apollo system since the television signal will be transmitted from the moon using an F.M. multiplex system.

APPENDIX I
COMPUTER PROGRAMS

PROGRAM	PURPOSE
VIDEO 3	Program which performs the actual calculation of points in the amplitude spectrum
BMTRX 6A	Typical program used for calculating the data points in B(x,y) and storing them on tape

```

PROGRAM VIDIOS
DIMENSION C(2), D(2), IC(2), IP(2)
COMMON IG00D,NTITLE(4),B(2400)
PI=3.1415927
R=WIND 2
DO 1 I=1,15
CALL BUFFIN3 (1)
CALL BUFFOUT3 (2)
1 CONTINUE
CALL UNLOAD (1)
R=WIND 2
READ 18, NRUNS
NPT=76840
N=M=150
DO 16 NRUN=1,NRUNS
READ 18, LPMIN,LPMAX,LQMIN,LQMAX
PRINT 19, (NTITLE(I),I=1,4),NPT,N,M,LPMIN,LPM
*AX,LQMIN,LQMAX
FM=N
EM=N
ICODE=1
DIV=2.0*EM*FM
DO 14 LP=LPMIN,LPMAX
PM1=LP-1
PAC=PI*PM1/EM
DO 13 LQ=LQMIN,LQMAX
QM1=LQ-1
QAC=PI*QM1/EM
SUMA=0.0
SUMB=0.0
PRINT 17, DIV,PAC,QAC
YK=0.
DO 7 III=1,15
CALL BUFFIN3 (2)
IF (III.EQ.15) 2,3
2 MAX=12
GO TO 4
3 MAX=20
4 DO 6 I=1,MAX
DO 5 J=1,270
XL=J-1
K=(I-1)*270+J
SUMA=SUMA+B(K)*COS(PAC*XL+QAC*YK)
SUMB=SUMB+B(K)*SIN(PAC*XL+QAC*YK)
5 CONTINUE
YK=YK+1.
6 CONTINUE
7 CONTINUE
PRINT 17, YK,SUMA,SUMB

```

```

      GO TO (8,9), ICODE
8.    I=1
      ICODE=2
      GO TO 10
9.    I=2
10   C(I)=((SUMA/DIV)**2+(SUMB/DIV)**2)**(1./2.)
      D(I)=20.*ALOG10(C(I))
      IQ(I)=LQ
      IP(I)=LP
      GO TO (12,11), I
11   ICODE=1
      PRINT 20, (IP(I),IQ(I),C(I),D(I),I=1,2)
12   REWIND 2
13   CONTINUE
14   CONTINUE
      NCOMP=(LPMAX-LPMIN+1)*(LQMAX-LQMIN+1)
      X=NCOMP/2
      Y=NCOMP
      Y=Y/2.
      IF (X.EQ.Y) 16,15
15   PRINT 20, IP(1),IQ(1),C(1),D(1)
16   CONTINUE
      STOP

C
17   FORMAT (3(10X,E15.8))
18   FORMAT (16I5)
19   FORMAT (1H1,10X,14HVIDI0 3 OUTPUT, //11X,4A4//
*11X,10HNPOINTS = ,I7/
*11X,4HN = ,I5, //11X,4HM = ,I5, //11X,8HP MIN =
*,I5,20X,8HP MAX = ,I5
*/11X,8HQ MIN = ,I5,20X,8HQ MAX = ,I5, //12X,2(
*1HP,4X,1HQ,7X,1HC,12X
*,6HLOG(C),10X),/)
20   FORMAT (1H ,8X,2(2I5,F13.5,2X,E13.5,4X))
      END

```

```
SUBROUTINE BUFFIN3 (I)
COMMON IGOOD,NTITLE(4),B(5400)
C THIS SUBROUTINE READS THE VARIABLES APPEARING
* IN THE COMMON
C STATEMENT FROM LOGICAL UNIT 1 (TAPE) IN A BIN
*ARY FORWARD READ
C MODE. A CHECKING SEQUENCE IS INCLUDED TO INSU
*RE THE TAPE INPUT
C PROCESS IS COMPLETED BEFORE CONTINUING AND TO
* DETECT ERRORS IN
C THE PROCESS.
ICOUNT=5
1 BUFFER IN (I,1) (IGOOD,B(5400))
2 GO TO (2,3,6,4), UNITSTF(I)
3 IF (IGOOD.EQ.99999) 7,1
4 ICOUNT=ICOUNT-1
IF (ICOUNT) 5,6,5
5 BACKSPACE I
GO TO 1
6 PRINT 8, I
STOP
7 RETURN
C
8 FORMAT (1H0,13HERROR ON UNIT,I6)
END
```

```
PROGRAM BMTRX6A1  
COMMON IGOOD,NTITLE(4),B(5400)
```

```
C  
C B MATRIX FOR GREY SCALE - LINEAR SCALE  
C MATRIX STORED ON ***** USER NUMBER 20 *****  
C BLACK=.01 - CONTRAST=100.  
C
```

```
BLACK=.01  
NTITLE(1)=4HBMTR  
NTITLE(2)=4HX 6A  
NTITLE(3)=4H1 OU  
NTITLE(4)=4HPUT  
M=1  
DO 9 I=1,292  
DO 1 J=1,39  
B(M)=BLACK  
1 M=M+1  
DO 2 J=40,77  
B(M)=.16666667  
2 M=M+1  
DO 3 J=78,116  
B(M)=.33333333  
3 M=M+1  
DO 4 J=117,154  
B(M)=.50000000  
4 M=M+1  
DO 5 J=155,193  
B(M)=.66666667  
5 M=M+1  
DO 6 J=194,231  
B(M)=.83333333  
6 M=M+1  
DO 7 J=232,270  
B(M)=1.0  
7 M=M+1  
IF (M.EQ.5401) 8,9  
8 CALL BUFFOUT3  
M=1  
9 CONTINUE  
CALL BUFFOUT3  
DO 10 I=1,10  
END FILE 1  
10 CONTINUE  
CALL UNLOAD (1)  
STOP  
END
```

```
SUBROUTINE PUFFOUT3
COMMON IGOOD,NTITLE(4),B(5400)
C THIS SUBROUTINE WRITES THE VARIABLES APPEARIN
C *G IN THE COMMON
C STATEMENT ON LOGICAL UNIT 1 (TAPE) IN A BINAR
C *Y MODE. A CHECKING
C SEQUENCE IS INCLUDED TO INSURE THE TAPE OUTPU
C *T PROCESS IS
C COMPLETED BEFORE CONTINUING AND TO DETECT ERR
C *ORS IN THE
C PROCESS.
1 IGOOD=99999
  ICOUNT=5
2 BUFFER OUT (02,1) (IGOOD,B(5400))
3 GO TO (3,7,4,4), UNITSTF(02)
4 ICOUNT=ICOUNT-1
  IF (ICOUNT) 5,6,5
5 BACKSPACE 2
  GO TO 2
6 BACKSPACE 2
  IGOOD=0
  BUFFER OUT (02,1) (IGOOD,B(5400))
  GO TO 1
7 RETURN
END
```

REFERENCES

1. Stanley Lebar and Charles Hoffman, "TV Show of the Century", Electronics, March 6, 1967.
2. R. C. Brainard, "Subjective Evaluation of PCM Noise-Feedback Coder for Television", Proceedings of I.E.E.E., March, 1967.
3. W. W. Harman, Principles of the Statistical Theory of Communications, Pages 115 - 116, McGraw Hill, New York, 1961.
4. John Hancock, The Principles of Communication Theory, Pages 175 - 176, McGraw Hill, New York, 1961.
5. V. K. Zworykin and G. A. Morton, Television, Pages 184 - 185, John Wiley & Sons, Inc., New York, 1954.
6. Glenn M. Glasford, Fundamentals of Television Engineering, Chapter 2, McGraw Hill, New York, 1955.
7. Jacob Millman and Herbert Taub, Pulse and Digital Circuits, Page 66, McGraw Hill, New York, 1956.
8. Harold A. Wheeler and Authur V. Loughren, "Fine Structure of Television Images", Proceedings of I.R.E., May, 1938.
9. L. E. Franks, "A Model for the Random Video Process", Bell System Technical Journal, April, 1966.
10. J. B. Chatten, R. G. Clapp, and D. G. Fink, "The Composite Video Signal -- Waveforms and Spectrum", I.R.E. Transactions on Broadcast and Television Receivers, July, 1955.
11. Pierre Mertz and Frank Gray, "A Theory of Scanning", Bell System Technical Journal, July, 1934.
12. R. W. Hamming, Numerical Methods for Scientists and Engineers, Chapter 6, McGraw Hill, New York, 1962.

P A R T II

TABLE OF CONTENTS

CHAPTER

I Gaussian Modulation

CHAPTER I
GAUSSIAN MODULATION

This section is concerned with the threshold of an ideal detector for Gaussian modulation. In order to determine if a phase-lock loop with an equivalent noise bandwidth equal to or greater than the pre-detection bandwidth behaves as Rice's "ideal" discriminator in the presence of noise, Rice's equations were numerically evaluated. Families of threshold curves were plotted, figure 1. The following is a discussion of the modification of Rice's equations such that equations pertain to a narrow band system, such as the Apollo Unified S Band FM system. Although some studies indicate the PLL, under the above bandwidth restraints, would behave as an ideal discriminator, the threshold curves obtained for Gaussian modulation and an ideal discriminator did not indicate this.

The noise power spectral density at the output of the ideal discriminator consists of a term due to impulses and one due to Gaussian noise and is given by

$$\omega_n(f) = 8\pi^2 (N_+ + N_-) + \frac{(2\pi f)^2}{Q^2} \omega_y(f)$$

N_+ = expected number of positive click events per second

N_- = expected number of negative click events per second

Q = carrier amplitude

$\omega_y(f)$ = power spectrum of the quadrature component of noise relative to the modulated carrier

$y = I_s(t) \cos \phi(t) - I_c \sin \phi(t)$ is the quadrature noise voltage.

The power spectrum of I_s and I_c is $2\omega_I(F + F_c)$ where $\omega_I(F)$ is the

noise power spectrum out of the IF filter. This spectrum is taken as

$$\omega_I(f) = \frac{bo}{\sqrt{2\pi}\sigma} e^{-(f - f_c)^2/2\sigma^2}$$

The spectra of I_c , I_s are bandpass white Gaussian processes. The Gaussian noise amplitude I_c , I_s are Rice's noise components representing the bandpass white noise I . $\phi(t)$ is the modulation. When the modulation is Gaussian the power spectrum of y , $\omega_y(f)$, is

$$\begin{aligned}\omega_y(f) &= 4 \int_0^{\infty} R_{IS}(\tau) e^{-F(\tau)} \cos 2\pi f \tau d\tau \\ R_{IS}(\tau) &= 2 \int_0^{\infty} \omega(f_c + f) \cos 2\pi f \tau df \\ F(\tau) &= \int_0^{\infty} \omega_{\phi}(f) \frac{(1 - \cos 2\pi f \tau)}{(2\pi f)^2} df\end{aligned}$$

$R_{IS}(\tau)$ is the autocorrelation of the noise component I_c and I_s are taken to be independent processes with zero mean and variance equal to the variance of the original noise process.

The autocorrelation function for the individual noise components is

$$\begin{aligned}R_{IS}(\tau) &= 2bo \int_0^{\infty} \frac{e^{-f^2/2\sigma^2}}{\sqrt{2\pi}\sigma} \cos 2\pi f \tau df \\ &= bo e^{-2\pi^2 \tau^2 \sigma_{IF}^2} \quad bo = R_{IS}(0)\end{aligned}$$

The function $F(\tau)$ is always positive and its relative magnitude determines the power spectrum of y . If $F(\tau) = 0$, the power spectrum of y would be just that of I_c , namely

$$\int_0^{\infty} R_{IS}(\tau) \cos 2\pi f \tau d\tau$$

It is not zero however, since its integrand is always positive. The actual spectrum of y depends on the two factors $R_{IS}(\tau)$ and $F(\tau)$. If $e^{-F(\tau)}$ goes to zero faster than $R_{IS}(\tau)$, the power spectrum of y increases over that of I_c . If the opposite is the case, then $\omega_y(f) \rightarrow \omega_I(f)$.

In order to determine the shape of $\omega_y(f)$ these two factors will be investigated.

For an equivalent rectangular bandwidth of 4MHz we have

$$\sigma_{IF} = \frac{4 \times 10^6}{\sqrt{2\pi}}$$

and

$$R_{IS}(\tau) = b_0 e^{-\pi(16 \times 10^{12})\tau^2}$$

so that for

$$\tau^2 = \frac{10^{-10}}{\pi(16)} \quad R_{IS}(\tau) \propto e^{-100} R_{IS}(0)$$

$$\tau = \frac{10^{-5}}{4\sqrt{\pi}} \approx 10^{-6}$$

The range of τ considered is then $0 < \tau < 10^{-6}$.

Consider the integrand of $F(\tau)$

$$G(f, \tau) = \frac{e^{-f^2/2\sigma_m^2} (1 - \cos 2\pi f \tau)}{\sqrt{2\pi} \sigma_m (2\pi f)^2}$$

For $\tau \leq 10^{-6}$, the integrand is dominated by the cutoff $\frac{e^{-f^2/2\sigma_m^2}}{(2\pi f)^2}$. As $\tau \rightarrow \infty$,

the integral diverges, but the factor $R_{IS}(\tau)$ cuts off the integral

for $\omega_y(f)$. The integrand of $F(\tau)$ is bounded for $\tau \leq 10^{-6}$. For F near 0,

$\frac{(1 - \cos 2\pi f \tau)}{(2\pi f)^2}$ may be expanded in a series to determine the maximum value of the integral i.e.,

$$\frac{1 - \cos 2\pi f \tau}{(2\pi f)^2} = \tau^2 \sum_{k=1}^{\infty} \frac{(2\pi f)^{2(k-1)} (-)^{k+1}}{2k!}$$

The first term is $\tau^2/2$. The integrand thus has a maximum value of

$$\frac{\tau^2}{2\sqrt{2\pi} \sigma_m} = \frac{10^{-18}}{2} \quad \text{at } f = 0$$

Then for f as large as 10^{12} , the integral is bounded by $F(\tau) < M = (10)^{12} 10^{-18} = 10^{-6}$ and $e^{-F(\tau)}$ is taken as 1. The power spectral density is

$$\omega_y(f) = 4 \int_0^{\infty} R_{IS}(\tau) \cos 2\pi f \tau d\tau$$

and

$$\omega_y(f) = \frac{1}{\sqrt{2\pi} \sigma} e^{-f/2\sigma^2}$$

The noise power due to the Gaussian noise component at the output of an ideal low pass filter of bandwidth $f_a = \frac{10^6}{2}$ is the integral of the power spectral density of equation (2) from 0 to f_a .

For Gaussian modulation, the number of positive click events per second is

$$N_+ = \frac{r}{\sqrt{\pi}} \int_0^{\infty} e^{-t^2} (1 + 2 a t^2)^{1/2} dt$$

and

$$a = \frac{\dot{\phi}^2}{(2\pi r)^2} \quad r = \sigma_{IF} \quad a = [BW_m / BW_{IF}]^2$$

Due to the assumption of symmetry in the modulation process, $N_+ = N_-$. The power density $8\pi (N_+ + N_-)$ assumes that N_+ and N_- are independent Poisson random variables. This is a flat spectrum across the low pass band for the case that $1/\delta < f_a$, where δ is the event duration.

The total output power is the integral of $\omega_n(f)$ of equation (1) over the low pass band $0 \leq f \leq f_a$.

The impulse noise power is evaluated as

$$N_1 = \int_0^{f_a} 8\pi^2 (N_+ + N_-) df = \frac{16\pi^2 f_a r}{\sqrt{\pi}} \int_0^{\infty} e^{-t^2} (1 + 2 a t^2) dt$$

The Gaussian noise power output is

$$N_2 = \int_0^{fa} \frac{2\pi^2}{\rho \sqrt{2\pi}} \sigma_{IF} f^2 e^{-f^2/2\sigma_{IF}^2} df$$

This becomes

$$N_2 = \frac{4\pi^2 \sigma_{IF}}{\rho \sqrt{2\pi}} \left[\frac{\sqrt{\pi}}{2} \sigma_{IF} \operatorname{erf} \left(\frac{fa}{\sqrt{2} \sigma_{IF}} \right) - fa e^{-fa^2/2\sigma_{IF}^2} \right]$$

which reduces to an asymptotic form normally seen when erf and the exponent are expanded in power series.

The output signal power is taken as

$$S_o = \frac{\pi^2 (BW_{IF})^2}{2} \quad BW_{IF} = \sqrt{2\pi} \sigma_{IF}$$

The signal to noise is then

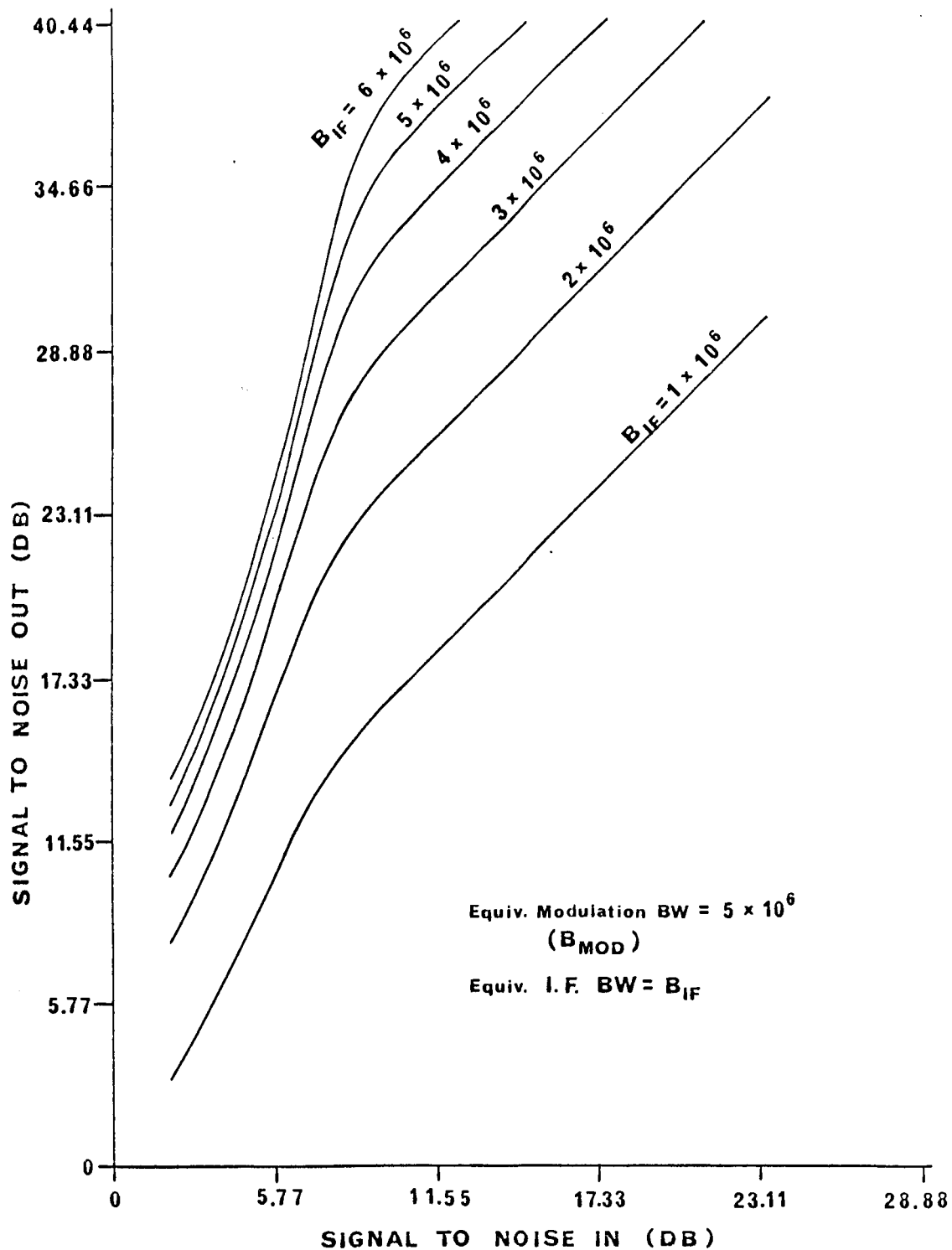
$$\left(\frac{S}{N_o} \right) = \frac{\pi^3 \sigma_{IF}^2}{\frac{16\pi^2 \sigma_{IF}^2 fa}{\sqrt{\pi}} \int_0^{\infty} e^{-t} (1 + 2 a t^2)^{1/2} dt + \frac{4\pi^2 \sigma_{IF}}{\rho \sqrt{2\pi}}}$$

$$\left[\frac{\sqrt{\pi}}{2} \sigma_{IF} \operatorname{erf} \left(\frac{fa}{\sqrt{2} \sigma_{IF}} \right) - fa e^{-fa^2/2\sigma_{IF}^2} \right]$$

For large ρ , the first term in the denominator becomes small and the ratio tends to the standard form

$$\left(\frac{S}{N_o} \right) = 3 \left(\frac{BW_{IF}}{BW_A} \right)^3 \rho$$

Figure (1) is a plot of equation (3) as σ_{IF} is varied.



$(S/N)_o$ vs $(S/N)_n$ AS A FUNCTION OF (B_{MOD}/B_{IF})
 FOR A GAUSSIAN MODULATION SPECTRUM

Figure 1